Journal of Physics A: Mathematical and Theoretical

PAPER

# Bulk-boundary correspondence in the quantum Hall effect

To cite this article: Andrea Cappelli and Lorenzo Maffi 2018 *J. Phys. A: Math. Theor.* **51** 365401

View the article online for updates and enhancements.

Related content

- Partition functions of non-Abelian quantum Hall states
  Andrea Cappelli and Giovanni Viola
- Matrix Effective Theories of the Fractional Quantum Hall effect
  Andrea Cappelli and Ivan D Rodriguez
- Central charge from adiabatic transport of cusp singularities in the quantum Hall effect
  Tankut Can

IOP ebooks™

Bringing you innovative digital publishing with leading voices to create your essential collection of books in STEM research.

Start exploring the collection - download the first chapter of every title for free.

This content was downloaded from IP address 130.229.169.153 on 26/07/2018 at 10:05

IOP Publishing Journal of Physics A: Mathematical and Theoretical

J. Phys. A: Math. Theor. **51** (2018) 365401 (31pp) https://doi.org/10.1088/1751-8121/aad0ab

# Bulk-boundary correspondence in the quantum Hall effect

**Andrea Cappelli**[1] **and Lorenzo Maffi**[1,2]

[1] Università di Firenze, Via G. Sansone 1, 50019 Sesto Fiorentino—Firenze, Italy
[2] Dipartimento di Fisica, Università di Firenze, Via G. Sansone 1, 50019 Sesto Fiorentino—Firenze, Italy

E-mail: andrea.cappelli@fi.infn.it

Received 24 January 2018, revised 26 June 2018
Accepted for publication 3 July 2018
Published 25 July 2018

**Abstract**

We present a detailed microscopic study of edge excitations for $n$ filled Landau levels. We show that the higher-level wavefunctions possess a non-trivial radial dependence that should be integrated over for properly defining the edge conformal field theory. This analysis let's us clarify the role of the electron orbital spin $s$ in the edge theory and to discuss its universality, thus providing a further instance of the bulk-boundary correspondence. We find that the values $s_i$ for each level, $i = 1, \ldots, n$, parameterize a Casimir effect or chemical potential shift that could be experimentally observed. These results are generalized to fractional and hierarchical fillings by exploiting the W-infinity symmetry of incompressible Hall fluids.

Keywords: quantum Hall effect, conformal field theory, Hall viscosity, W-infinity symmetry

(Some figures may appear in colour only in the online journal)

## 1. Introduction

The geometric response [1] of quantum Hall states [2] has been extensively investigated in the recent literature [3, 4]. The low-energy effective action has been extended by coupling to a background metric, leading to the Wen–Zee terms [5, 6]. Other methods have also been developed, such as explicit wavefunction constructions [7, 8], hydrodynamic theory [9], the W-infinity symmetry [10], and bi-metric theories [11].

As in any topological phase of matter, the responses have a dual manifestation in the bulk and at the edge of the system, and their interplay is called the bulk-boundary correspondence [2]. The best-known example is given by the electromagnetic response: the bulk Hall current compensates the chiral anomaly at the edge, i.e. the non-conservation of the boundary charge, according to the so-called anomaly inflow mechanism [12] (also known as Laughlin

 © 2018 IOP Publishing Ltd Printed in the UK 

flux argument [13]). Since the anomaly is an exact and universal feature of the conformal field theory of edge excitations [14, 15], and is related to topological invariant quantities, we can infer that the bulk Hall conductivity $\sigma_{\rm H}$ is also universal and exact.

The first geometric response of the edge theory is given by the gravitational anomaly parameterized by the difference of conformal central charges $c - \bar{c}$ of chiral and anti-chiral edge modes (in the simplest case $\bar{c} = 0$). This anomaly describes the thermal Hall current and thermal conductivity $\kappa_{\rm H}$ [15], recently observed experimentally [16], and its value is similarly exact and universal. The bulk-boundary correspondence is more subtle in this case, since the heat current flows on the edges and not in the bulk [17]. Other bulk effects parameterized by $c$ have nevertheless been recently found, using effective actions [18], Berry phase calculations [7, 8] and hydrodynamic approaches [9].

In this paper we analyze the second geometric response involving the electron orbital spin $s$ (intrinsic angular momentum) and describe the associated bulk-boundary correspondence. Originally introduced in the Wen–Zee action, the quantity $s$ parameterizes several interesting bulk phenomena: a shift in the linear relation between the number of electrons and fluxes for compact spatial geometries [5], the response of the Hall fluid to shear, i.e. the Hall viscosity [1, 3, 4], the spatial modulation of the Hall current [19] and, finally, the fluctuation of the ground-state density near the edge [20]. Furthermore, the combination $c - 12\nu s^2$ parameterizes the Berry phase of the ground-state [7].

Since $s$ is a coupling constant of an action of Chern–Simons type, it is independent of local dynamics and universal for translation invariant systems. Moreover it is associated to a topological quantity in compact geometries. However, it is not related to an anomaly of the edge theory, and its physical meaning at the edge has so far remained unclear.

The recent work [21] has shown that in geometries with a boundary, the Wen–Zee action is modified by the addition of two boundary terms parameterized by the orbital spin, that are local edge actions and thus non-anomalous. This result implies that the Hall fluid can have interfaces where the averages over electron species $\bar{s}$ and $\overline{s^2}$ change values without breaking any symmetry or closing the gap. In the disc geometry, these local terms also predict ground-state values of the charge and conformal spin at the edge.

In this paper, we describe the role of the orbital spin within edge physics and explain the universal features that can be associated to this quantity. We first build the theory of edge excitations for $n$ filled Landau levels, by taking a straightforward limit of the microscopic states near the edge. This analysis was not done in the past beyond the lowest level $n = 0$ [12], to the best of our knowledge, and is relevant for our problem, because the orbital spin takes different values, $s_i = (2{\rm i} + 1)/2$ in the levels $i = 0, 1, \ldots, n - 1$. We consider the geometry of the disc with radius $R$, realized by the infinite plane with a confining potential; we find that the edge states are localized at values of the radius $r \sim R$, and for $i > 0$ rapidly oscillate in a region of the size of the magnetic length, $|r - R| = \Delta$ with $\Delta = O(\ell)$. We then define the edge currents $\rho^{(i)}(\theta)$ that are bilinears of Fermi fields and obtain the chiral conformal field theory (Luttinger theory) with $n$ independent branches and central charge $c = n$ [2].

Next we discuss the edge spectrum and show that the $s_i$ cause a shift in the dispersion relation, up to a global constant, $s_i \to s_i + s_o$, that is independent of bulk dynamics. The $s_i$ can be included in the Hamiltonian of the conformal theory, i.e. the Virasoro generator $L_0$, by a redefinition of the chemical potential $\mu_i \to \mu_i - s_i$ that becomes level dependent.

We describe some physical consequences of this fact in several settings at the edge. In the general case of smooth boundary and non-interacting branches of excitations, this effect is not observable. In the case of a disc with a sharp boundary, and for interacting branches, we find non-vanishing ground-state values of the edge charge and conformal spin that are

parameterized by the differences $s_i - s_j$, and are in agreement with the results of the effective action approach [21]. These are Casimir-like effects associated to the orbital spin. Note that ground-state values of relativistic theories are not observable in general, but relative differences do make sense.

In the second part of this work, we show how to generalize these results to fractional fillings $\nu < 1$ by using the W-infinity symmetry of incompressible Hall fluids [22–24]. Namely, we describe the edge excitations by deforming the density with area-preserving diffeomorphisms of the plane. We thus recover the edge expansion at $r \sim R$ with its radial dependence characterizing the different branches. In particular, the Jain hierarchical states with $\nu = n/(qn+1)$, $q$ even, possess $n$ branches of edge states with orbital spins $s_i = i + (q+1)/2$, $i = 0, \ldots, n-1$, corresponding again to $s_i - s_j \in \mathbb{Z}$. These quantities parameterize the ground-state values of edge charge and conformal spin.

In last section, we briefly discuss the possibility of measuring these effects by a tunneling experiment in the Coulomb blockade regime [25] and by quadrupole deformation of the confining potential [26].

The outline of the paper is as follows. In section 2, we recall some facts about the Wen–Zee action and the results of [21] concerning the orbital spin at the boundary. In section 3 we perform the microscopic derivation of the edge conformal theory for $n$ filled Landau levels. In section 4, we describe the physical consequences of the orbital spin. In section 5, we reobtain the multicomponent edge theory by using the W-infinity transformations of the bulk and extend the analysis of orbital spin effects to fractional fillings. In section 6, we discuss possible experiments. Finally, the conclusions present some remarks and open problems. The two appendices contain the analysis of non-relativistic corrections to the conformal theory and the calculation of the Landau level spectrum with general boundary potential.

## 2. Effective actions and geometric response

In this section, we introduce the effective action of quantum Hall states, in the multicomponent case that will be relevant for the following analysis [2]. The geometric part of the action, not involving any local dynamics, can be derived by assuming that the low-energy fluctuations of the incompressible fluid are described by conserved currents $j^\mu_{(i)}$, that are dual to hydrodynamic gauge fields $a_{(i)\nu}$, $\mu, \nu = 0, 1, 2$, as follows:

$$j^\mu_{(i)} = \frac{1}{2\pi}\varepsilon^{\mu\nu\rho}\partial_\nu a_{(i)\rho}, \qquad i = 0, \ldots, n-1, \tag{2.1}$$

for any component $(i)$. The gauge fields interact by a Chern–Simons topological action, with couplings specified by the so-called $K$ matrix. The system is placed in an electromagnetic background $A_\mu$ and a (time-dependent) spatial metric $g_{ij}$, $i,j = 1,2$, whose associated spin connection is Abelian, $\omega_\mu = \varepsilon_{ab}\omega^{ab}_\mu/2$, where $a, b = 1, 2$ are local frame indices [7]. Using the notation of forms, i.e. $a = a_\mu \mathrm{d}x^\mu$, and summing over the $n$ fluid components, we write the following effective action:

$$S[a, A, \omega] = -\frac{1}{4\pi}\int K_{(i)(j)}a_{(i)}\mathrm{d}a_{(j)} + \frac{1}{2\pi}\int a_{(i)}\left(t_{(i)}\mathrm{d}A + s_{(i)}\mathrm{d}\omega\right), \tag{2.2}$$

where $t_{(i)}$ are the charges of fluid components (conventionally, $t_{(i)} = 1 \ \forall i$) and $s_{(i)}$ are their orbital spin values.

The integration over the $a_{(i)}$ field yields the induced action [6],

$$S_{\rm ind}[A,g] = \frac{\nu}{4\pi}\int \left( A{\rm d}A \;+\; 2\bar{s}\;\omega{\rm d}A \;+\; \overline{s^2}\;\omega{\rm d}\omega \right) \;+\; \frac{c}{96\pi}\int {\rm Tr}\left(\Gamma{\rm d}\Gamma + \frac{2}{3}\Gamma^3\right), \tag{2.3}$$

with the following expressions for the parameters [2]:

$$\nu = t_{(i)}K^{-1}_{(i)(j)}t_{(j)}, \qquad \nu\bar{s} = s_{(i)}K^{-1}_{(i)(j)}t_{(j)}, \qquad \nu\overline{s^2} = s_{(i)}K^{-1}_{(i)(j)}s_{(j)}, \qquad c = n, \tag{2.4}$$

corresponding to the filling fraction $\nu$, the average orbital spin $\bar{s}$, the average square $\overline{s^2}$ and the central charge $c$, respectively. The conventional naming for these quantities refers to the case of integer filling, where $K$ is the identity matrix (we only discuss the case of positive definite $K$, for simplicity). The $s_{(i)}$ values for $\nu = n$ can be computed from the total angular momentum $M$ of each level filled with $N$ electrons, using the formula:

$$M = \frac{N^2}{2\nu} - Ns, \tag{2.5}$$

where $\nu = 1$ for each level. One finds:

$$s_{(i)} = \frac{2i+1}{2}, \qquad i = 0,\ldots,n-1. \tag{2.6}$$

In the expression of the induced action (2.3), the first term is the Chern–Simons form $S_{\rm CS}$ responsible for the Hall conductance, and the second and third terms are called Wen–Zee $S_{\rm WZ}$ and gravitational Wen–Zee terms $S_{\rm gWZ}$, respectively. The last term, the gravitational Chern–Simons term $S_{\rm gCS}$, involves the Christoffel connection $(\Gamma)^\mu_\nu = \Gamma^\mu_{\nu\lambda}{\rm d}x^\lambda$ and arises from the measure of integration for the $a_{(i)}$ path-integral, owing to the framing anomaly [27].

In a spatial geometry $\Sigma$ with a boundary, like the disk $D_2$, the action (2.3) is invariant under gauge transformations and diffeomorphisms up to total derivatives that must be compensated by additional boundary terms. The solution of this problem is well-known and leads to the existence of massless edge excitations described by a conformal field theory defined on the spacetime boundary of the cylinder $\partial\mathcal{M} = S_1 \times \mathbb{R}$ [2]. In the present discussion, this is given by the so-called Abelian theory of $n$ chiral massless bosonic fields $\varphi_{(i)}$ (chiral Luttinger theory), with action $S_{\rm CFT}[\varphi_{(i)}, A, g]$, also involving the coupling to the $A$ and $g$ backgrounds. It can be shown that the variation of $S_{\rm CFT}$ under gauge transformations and diffeomorphisms cancels the corresponding variations of the two terms $S_{\rm CS}$ and $S_{\rm gCS}$ in the bulk action, respectively.

The conformal theory at the edge is characterized by chiral and gravitational anomalies; the first one corresponds to the non-conservation of the edge charge and matches the bulk Hall current by the anomaly inflow mechanism [12]. The gravitational anomaly amounts to non-conservation of energy-momentum in the cylinder and leads to the heat current. These anomalies cannot be eliminated by adding terms in the action that are local in two dimensions, the spacetime where the conformal theory is defined. Actually they are compensated by actions that are local in one extra dimension, $S_{\rm CS}$ and $S_{\rm gCS}$, that are thus uniquely determined. Furthermore, the anomalies are exact quantities in the conformal theory that are independent of short-distance physics [14]. These results ensure that the coefficients $\nu$ and $c$, respectively parameterizing the electric and thermal conductance $\sigma_{\rm H}$ and $\kappa_{\rm H}$, are universal quantities independent of the details of the system. This is the bulk-boundary correspondence associated to these responses.

Next, we discuss the boundary terms needed to correct the non-invariances of the second and third terms, $S_{\rm WZ}$ and $S_{\rm GRWZ}$ in the action (2.3). They have been recently found in [21] and read:

$$S_{\mathrm{WZ,b}} = \frac{\nu\bar{s}}{2\pi}\int_{\partial\mathcal{M}} AK, \qquad S_{\mathrm{gWZ,b}} = \frac{\nu\overline{s^2}}{4\pi}\int_{\partial\mathcal{M}} \omega K, \tag{2.7}$$

where the integrals are taken on the boundary cylinder, $A$ and $\omega$ are the restrictions of the one-forms on the boundary and $K$ is the one-form of the extrinsic curvature of the boundary, $K = K_\alpha \mathrm{d}x^\alpha$, $\alpha = 0, 1$.

The expressions (2.7) are local in $(1+1)$ dimensions and thus are not related to an anomaly of the edge theory. In generic quantum field theories, local terms of the action are not universal in the sense that they depend on the dynamics and can be modified, according to different (possible) definitions of the renormalized quantities. Actually, the local terms (2.7) can also be considered for an interface between two regions where $\bar{s}$ and $\overline{s^2}$ take different values in the bulk [21]. At this point the gap does not vanish and there are no edge excitations. In conclusions, the results (2.7) suggest that the average orbital spin and its square average are not universal quantities on the edge as well as in the bulk in absence of translation invariance.

Summarizing, the effective action for the disk geometry is given by the equations (2.3) and (2.7):

$$S_{\mathrm{ind}}[A, g] = S_{\mathrm{CS}} + S_{\mathrm{WZ}} + S_{\mathrm{WZ,b}} + S_{\mathrm{gWZ}} + S_{\mathrm{gWZ,b}} + S_{\mathrm{gCS}} + S_{\mathrm{CFT}}. \tag{2.8}$$

The induced currents and response coefficients are found by taking variations of this action, as reviewed e.g. in [10]. Let us mention two results that are useful for the following analysis:

- The total number of particles is given by the space integral of the density, $\sqrt{g}\rho_0 = \delta S_{\mathrm{ind}}/\delta A_0$, and reads:

$$\begin{aligned} N &= \frac{\nu}{2\pi}\int_\Sigma \sqrt{g}B \;+\; \frac{\nu\bar{s}}{4\pi}\int_\Sigma \sqrt{g}\mathcal{R} \;+\; \frac{\nu\bar{s}}{2\pi}\int_{\partial\Sigma} k + Q_{\mathrm{CFT}} \\ &= \nu N_\phi + \nu\bar{s}\chi + Q_{\mathrm{CFT}}. \end{aligned} \tag{2.9}$$

  In this expression, there appear the scalar curvature, $\mathcal{R} = 2\varepsilon^{ij}\partial_i\omega_j/\sqrt{g}$, the number $N_\phi$ of magnetic fluxes through the surface and the Euler characteristic $\chi$. Note that the bulk and boundary terms $S_{\mathrm{WZ}}$ and $S_{\mathrm{WZ,b}}$ in the action combine themselves to give the correct expression of the Gauss–Bonnet theorem for surfaces with a boundary, including the geodesic curvature $k$, leading to $\chi = 2 - 2h + b$, where $h$ and $b$ are the number of handles and boundaries, respectively.
- The spin density can be obtained by the variation of the action with respect to the spin connection at fixed metric, $\sqrt{g}s^0 = \delta S_{\mathrm{ind}}/\delta\omega_0|_g$. There is an ambiguity in performing this derivative, because metric and spin connection are independent variables only in presence of torsion, that was not fully accounted for in the derivation of (2.3). At any rate, this ambiguity amounts to trading angular momentum for spin. We are interested in the boundary contribution that originates from the term $S_{\mathrm{gWZ,b}}$ (2.7) for the geometry of the flat disk ($\chi = 1$). It reads:

$$\mathcal{S}_{\mathrm{b}} = \int_{S_1} s^0 = \frac{\nu\overline{s^2}}{4\pi}\int_0^{2\pi R} \mathrm{d}x\, k = \frac{\nu\overline{s^2}}{2}. \tag{2.10}$$

Summarizing, in the geometry of the disk, the Wen–Zee action supplemented by the boundary terms (2.7) predicts non-vanishing ground-state values for the spin (2.10) and the charge,

$$Q_{\mathrm{b}} = \nu\bar{s} + Q_{\mathrm{CFT}}, \tag{2.11}$$

at the boundary. In section 4, we shall recover and extend these results by studying the edge conformal theory and explain to which extent these quantities are universal.

## 3. Multicomponent edge theory

In this section we find the conformal theory of edge excitations by taking a suitable limit of the microscopic states of $n$ filled Landau levels. This result will set the stage for the analyses in this paper. Although the limit to the edge is rather straightforward, it was not yet analyzed in the literature, beside the one-component case of the lowest Landau level of [12] and the nice work [28].

We consider the Landau levels in the infinite plane with symmetric gauge as discussed in [12] and adopt the notations of that paper. In particular, the magnetic length $\ell = \sqrt{2\hbar c/eB}$, $c$, $e$, $\hbar$ and the electron mass $m$ are set to one, corresponding to $B = 2$. The Hamiltonian and angular momentum take the form:

$$H = 2a^\dagger a + 1, \qquad J = b^\dagger b - a^\dagger a, \tag{3.1}$$

in terms of two pairs of mutually commuting creation-annihilation operators,

$$\begin{aligned} a &= \frac{z}{2} + \overline{\partial}, \qquad a^\dagger = \frac{\overline{z}}{2} - \partial, \qquad \left[a, a^\dagger\right] = 1, \\ b &= \frac{\overline{z}}{2} + \partial, \qquad b^\dagger = \frac{z}{2} - \overline{\partial}, \qquad \left[b, b^\dagger\right] = 1, \end{aligned} \tag{3.2}$$

involving the complex coordinate of the plane, $z = r\exp(\mathrm{i}\theta)$. The single particle wavefunctions $\psi_{n,m}(z,\overline{z})$ are characterized by the values of the level index $n = 0, 1, \ldots$ and angular momentum $m = -n, -n+1, \ldots$. Their expression is:

$$\begin{aligned} \psi_{n,m} &= \frac{\left(b^\dagger\right)^{n+m}}{\sqrt{(n+m)!}} \frac{\left(a^\dagger\right)^n}{\sqrt{n!}} \frac{1}{\sqrt{\pi}} \mathrm{e}^{-|z|^2/2} \\ &= \sqrt{\frac{n!}{\pi\,(n+m)!}} z^m L_n^m\left(|z|^2\right) \mathrm{e}^{-|z|^2/2}, \qquad m + n \geqslant 0, \end{aligned} \tag{3.3}$$

where $L_n^m$ are the generalized Laguerre polynomials.

### 3.1. Limit of wavefunctions to the edge

We consider the Hall state made by filling up to $N$ electrons per level, thus forming a droplet of fluid of radius $R^2 \sim N$, due to the flux/degeneracy relation. A confining radial potential breaks the degeneracy of Landau levels near the boundary and create a Fermi surface around that point. The specific form of the potential will be discussed later and is not relevant momentarily.

The edge theory is defined by the states that describe particle-hole excitations around the Fermi surface in a finite range of energy, i.e. of angular momentum, in the limit $R \to \infty$. The states in the $i$th Landau level, $i = 0, 1, \ldots$, filled with $N$ electrons have momenta $-i \leqslant m < N - i$. The edge theory is defined in the range [12]:

$$L - \sqrt{L} < m < L + \sqrt{L}, \qquad L \equiv R^2 \to \infty, \tag{3.4}$$

where $L \sim N$ is a given common momentum near the Fermi surface and the range of $m$ is chosen to fit a linear spectrum of edge energies, $\varepsilon_m \sim v(m - L)/R$, i.e $\varepsilon(k) = vk$ with $k$ the one-dimensional momentum.

As is well known, the wavefunctions $|\psi_{n,m}(r)|$ are localized around the semiclassical orbits with $r^2 \sim m$. Thus, we can also expand the edge states for $r \sim R$ and consider the combined limit for the angular momentum (3.4) and the radial coordinate,

$$r = R + x, \qquad x = O(1), \qquad R \to \infty. \tag{3.5}$$

Let us perform this limit on the functions of the first level $n = 0$: we redefine the momentum w.r.t. the Fermi surface $m = L + m'$ and use the Stirling expansion. We obtain:

$$\psi_{0,L+m'}(r,\theta) \simeq \mathcal{N}\frac{\mathrm{e}^{\mathrm{i}\left(L+m'\right)\theta}}{\sqrt{2\pi R}}\,\mathrm{e}^{-\left(x-\frac{m'}{2R}\right)^2}\left(1+O\left(\frac{1}{R},\frac{m'}{R^2}\right)\right),$$
$$r = R + x, \qquad x = O(1), \qquad |m'| \leqslant R, \qquad R^2 = L \to \infty, \tag{3.6}$$

where the normalization constant is $\mathcal{N} = (2/\pi)^{1/4}$. These wavefunctions are plotted in figure 1(a).

In the expression (3.6), the first factor corresponds to the wavefunction $\psi_{m'}(\theta) = \mathrm{e}^{\mathrm{i}m'\theta}/\sqrt{2\pi R}$ for the $(1+1)$-dimensional Weyl fermion of the edge theory, while the radial part is peaked at $r \sim R$ with spread $O(\ell)$ for $R \to \infty$. In the earlier work [12], the states of the edge theory were thus identified with the wavefunctions at fixed radius $x = 0$, the remaining cut-off in momentum $\exp(-(m'/2R)^2)$ being irrelevant for $R \to \infty$.

It turns out that neglecting the radial dependence is not appropriate for higher Landau levels. In order to understand the problem, let us consider the form of the second level wavefunctions:

$$\psi_{1,m} = \frac{z^m}{\sqrt{\pi\,(m+1)!}}\left(r^2 - m - 1\right)\mathrm{e}^{-r^2/2}. \tag{3.7}$$

Upon taking the limit to the edge, we find:

$$\psi_{1,L+m'-1} \simeq \mathcal{N}\frac{\mathrm{e}^{\mathrm{i}\left(L+m'-1\right)\theta}}{\sqrt{2\pi R}}\,2\left(x-\frac{m'}{2R}\right)\mathrm{e}^{-\left(x-\frac{m'}{2R}\right)^2}. \tag{3.8}$$

The radial function now shows an oscillation of size $x = O(1)$ near the edge, as shown in figure 1(b).

The oscillating behaviour is also present in the higher levels, for the simple reason that the wavefunctions should be orthogonal among themselves at fixed angular momentum, i.e. in $r$ space. Owing to the Gaussian factor, it is rather easy to guess that the radial functions should map into the harmonic oscillator basis involving the Hermite polynomials $H_n$. This is indeed the case: in equation (3.8), the polynomial is identified as $(x - m'/(2R)) \sim H_1(x - m'/(2R))$. The inspection of the next few cases leads to the following result:

$$\psi_{n,L+m}(R+x,\theta) \simeq \mathcal{M}\frac{\mathrm{e}^{\mathrm{i}(m+L)\theta}}{\sqrt{2\pi R}}H_n\left[\sqrt{2}\left(x-\frac{m+n}{2R}\right)\right]\mathrm{e}^{-\left(x-\frac{m+n}{2R}\right)^2}, \tag{3.9}$$

where $\mathcal{M}$ is another normalization factor.

The shift of the radial coordinate by $m/2R$ in (3.9) is also easily explained. In the limit $R \to \infty$, the disk geometry can be approximated by the half plane, defined by $x < 0$ in $(x, y)$ coordinates. In this geometry, the Landau levels in the linear gauge $(A_x, A_y) = (0, Bx) = (0, 2x)$ have the form:

$$\widetilde{\psi}_{n,k_y}(x,y) \sim \mathrm{e}^{\mathrm{i}k_y y}H_n\left[\sqrt{2}\left(x-\frac{k_y}{2}\right)\right]\mathrm{e}^{-\left(x-\frac{k_y}{2}\right)^2}. \tag{3.10}$$

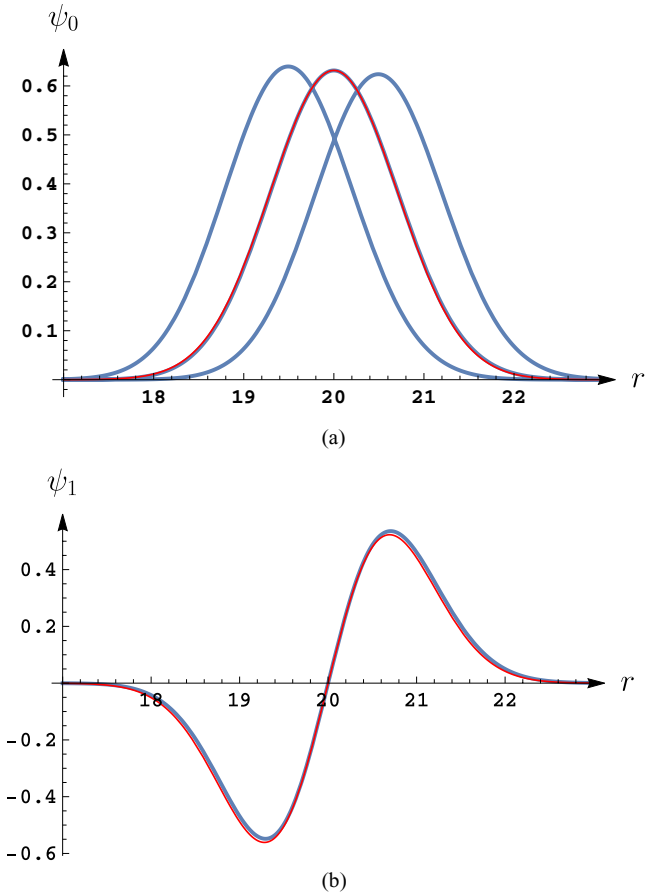


**Figure 1.** (a) Radial dependence of $\psi_{0,L+m'}$, for $L = R^2 = 400$ and $m' = \{-20, 0, 20\}$ (blue), and its leading approximation (3.6) (red), for $m' = 0$. (b) Radial dependence of $\psi_{1,L-1+m'}$ (blue) and its approximation (3.8) (red), for $L = R^2 = 400$ and $m' = 0$.

Owing to the periodicity of the edge of the disk, the half plane is wrapped in the $y$ direction to form a cylinder, such that the corresponding momentum is quantized by $k_y = m/R$. We thus recover the expression (3.9) up to an overall phase for the different gauge choice.

Note, however, that the functions (3.10) for the cylinder match those of the disk (3.9) with a level-dependent shift of momentum $m/R \to (m+n)/R$ that will be crucial in the following discussion. This difference is due to the extrinsic curvature of the boundary of the disc, that vanishes for the half-plane and cylinder geometries. This is a first instance of the orbital spin $s_n$ in the edge theory.

In conclusion, the wave functions of edge states are Gaussians localized in a spatial region $O(\ell)$ around $r = R$ and a momentum range $O(\sqrt{L})$ around $L = R^2$. The spatial separation $\Delta x = 1/2R$ between neighbor states is in agreement with the degeneracy/flux relation, since $N_\phi \to N_\phi + 1$ amounts to $R^2 \to (R + 1/2R)^2 \sim R^2 + 1$. The states of higher Landau level display an oscillating radial dependence that is required by orthogonality. A glimpse of this fact had already appeared in analysis of density shapes of [28].

### 3.2. Multicomponent conformal theory

We now construct the conformal theory of Weyl fermions that describes the edge excitations for $\nu = n$. The strategy is to consider bilinears of Fermi fields that are observable quantities, in particular the modes of the density $\hat{\rho}_k$ that are the building blocks of the Abelian conformal theory [14].

Let us start from the second-quantized field operator for $n$ Landau levels,

$$\hat{\Psi}(z,\bar{z}) = \sum_{m=0}^{\infty} \psi_{0,m}\hat{c}_m^{(0)} + \sum_{m=-1}^{\infty} \psi_{1,m}\hat{c}_m^{(1)} + \ldots + \sum_{m=-n+1}^{\infty} \psi_{n-1,m}\hat{c}_m^{(n-1)}, \tag{3.11}$$

where $\hat{c}_m^{(i)}$ are fermionic destruction operator. We consider the density, $\hat{\rho}(z,\bar{z}) = \hat{\Psi}^\dagger\hat{\Psi}$, and analyze the Fourier modes at the edge, also integrating over the radial coordinate:

$$\hat{\rho}_k \equiv \int_0^\infty \mathrm{d}r\, r \int_0^{2\pi} \mathrm{d}\theta\, \hat{\rho}(r,\theta)\, \mathrm{e}^{-\mathrm{i}k\theta}. \tag{3.12}$$

This expression is analyzed in the limit to the edge of the previous section, namely $R \to \infty$ with $r = R + x$, $x = O(1)$, $R^2 = L$, $m = L + m'$, $|m'| < \sqrt{L}$. First we substitute the field expansion (3.11):

$$\begin{aligned}\hat{\rho}_k = \int_{-R}^{\infty} (R+x)\,\mathrm{d}x \int_0^{2\pi} \mathrm{d}\theta \sum_{m,n} \Big(\psi_{0,L+m}(x,\theta)\,\hat{d}_m^{(0)} + \psi_{1,L+m}(x,\theta)\,\hat{d}_m^{(1)} + \ldots\Big) \\ \times \Big(\psi^*_{0,L+n}(x,\theta)\,\hat{d}_n^{(0)\dagger} + \psi^*_{1,L+n}(x,\theta)\,\hat{d}_n^{(1)\dagger} + \ldots\Big)\,\mathrm{e}^{-\mathrm{i}k\theta},\end{aligned} \tag{3.13}$$

having redefined $\hat{d}_m^{(i)} \equiv \hat{c}_{L+m}^{(i)}$. We then take the edge limit on wavefunctions and use the orthogonality of Hermite polynomials; to leading order $O(1)$ in the $1/R$ expansion, we find:

$$\begin{aligned}\hat{\rho}_k &= \sum_{m\in\mathbb{Z}} \Big(\hat{d}_{m-k}^{(0)\dagger}\hat{d}_m^{(0)} + \hat{d}_{m-k}^{(1)\dagger}\hat{d}_m^{(1)} + \hat{d}_{m-k}^{(2)\dagger}\hat{d}_m^{(2)} + \ldots\Big) + \mathcal{O}\left(\frac{1}{R},\frac{k}{R}\right) \\ &= \hat{\rho}_k^{\mathrm{CFT}(0)} + \hat{\rho}_k^{\mathrm{CFT}(1)} + \hat{\rho}_k^{\mathrm{CFT}(2)} + \ldots + \mathcal{O}\left(\frac{1}{R},\frac{k}{R}\right).\end{aligned} \tag{3.14}$$

In this calculation we neglected the shifts in the coordinates, $x - \Delta m/R \sim x$, corresponding to the underlying low-momentum expansion.

The result (3.14) shows that the edge Fourier modes of the two-dimensional charge decompose into $n$ independent contributions $\hat{\rho}_k^{\mathrm{CFT}(i)}$, $i = 0,\ldots,n-1$, that act on the Fock spaces of the respective Landau levels. Their expressions match the fermionic representation of the multicomponent Abelian conformal theory with $c = n$. This result also agrees with the effective theory approach of section 2, where the edge fields $\varphi^{(i)}$ realize the bosonic representation of the same conformal theory, i.e. $\hat{\rho}^{\mathrm{CFT}(i)}(\theta) = \partial_\theta\varphi^{(i)}(\theta)$ [2].

Therefore, the $n$ edge densities are obtained by radial integration of the bulk density in the limit $R \to \infty$. More precisely, the edge states are found by averaging the radial dependence of microscopic states near the edge in a shell $R - \Delta < r < R + \Delta$, with $\Delta = O(1)$, i.e. of the size of the ultraviolet cutoff. Other observables of the conformal theory are similarly obtained by radial integration of bilinear bulk quantities. For example, the edge correlator is defined by:

$$\langle\psi(\theta)\psi^\dagger(\theta')\rangle_{\mathrm{CFT}} \simeq \int \mathrm{d}r\; r\; \langle\Omega|\Psi(r,\theta)\Psi^\dagger(r,\theta')|\Omega\rangle. \tag{3.15}$$

This expression also decomposes in independent contributions for each branch of edge excitations.

In conclusion, the $n$ edge densities are obtained by radial integration of the bulk density in the limit $R \to \infty$. More precisely, the edge states are found by averaging the radial structure of microscopic states near the edge in a shell $r - R = O(1)$, i.e. of the size of the ultraviolet cutoff. Note that no non-locality is introduced by this approach, that is simply a low-energy expansion.

Next, we observe that the contribution of one level can be single out from the total current (3.12) by integrating in $r$ with a suitable weight function $f_j(r)$, and using the orthogonality of Hermite polynomials. For example, let us suppose that we would like to remove the contribution of the lowest level $\hat{\rho}_0^{(0)}$ from the sum (3.14). We can use the weight,

$$f_{(0)}(x) = 1 - 4x^2, \tag{3.16}$$

and compute $\hat{\rho}'_k = \int \mathrm{d}^2 x f_{(0)} \hat{\rho}(r,\theta) \mathrm{e}^{-\mathrm{i}k\theta}$. We find that the lowest level does not contribute to leading order $O(1)$, because:

$$\int_{-\infty}^{\infty} \mathrm{d}r r f_{(0)}\, \varphi_{0,L+m}\, \varphi^*_{0,L+m+k} = O\left(\frac{1}{R}\right). \tag{3.17}$$

The fact that the Abelian currents appear at leading order $O(1)$ in the $R \to \infty$ expansion is expected for conformal theories on the spacetime cylinder [14]. Higher orders $O(1/R^k)$ correspond to conserved currents of higher spin/conformal dimension $h = k + 1$.

### 3.3. Conformal field theory of Weyl fermions and ground-state conditions

We now recall some basic facts of the free chiral fermionic theory on the geometry of the spacetime cylinder. The Virasoro and current modes are written in terms of fermionic Fock space operators as follows [12],

$$\hat{L}_n = \sum_{k=-\infty}^{\infty} \left(k - \frac{n}{2} - \mu\right) : \hat{d}^\dagger_{k-n} \hat{d}_k :, \tag{3.18}$$

$$\hat{\rho}_n = \sum_{k=-\infty}^{\infty} : \hat{d}^\dagger_{k-n} \hat{d}_k :, \tag{3.19}$$

where the normal ordering $: () :$ subtracts the infinite contribution of the Dirac sea. Let us conventionally fill the sea up to the $k = 0$ state [12], i.e. define the conformal theory ground-state by the conditions:

$$\begin{aligned} \hat{d}_k |\Omega, \mu\rangle &= 0, \qquad k > 0, \\ \hat{d}^\dagger_k |\Omega, \mu\rangle &= 0, \qquad k \leqslant 0. \end{aligned} \tag{3.20}$$

Thus, the normal ordering is defined by putting $\hat{d}_k$ to the right of $\hat{d}^\dagger_k$ for $k > 0$ and viceversa for $k \leqslant 0$. The commutation relations of Virasoro and current modes (3.18) and (3.19) are then obtained from those of the Fock space, with the result [12]:

$$\begin{aligned} &[\hat{\rho}_n, \hat{\rho}_m] = n\delta_{n+m,0}, \\ &\left[\hat{L}_n, \hat{\rho}_m\right] = -m\hat{\rho}_{n+m}, \\ &\left[\hat{L}_n, \hat{L}_m\right] = (n-m)\hat{L}_{n+m} + \frac{1}{12}\left(n^3 - n\right)\delta_{n+m,0}. \end{aligned} \tag{3.21}$$

This is the well-known current algebra with central charge $c = 1$ [14].

The Hamiltonian of the conformal theory on the cylinder is expressed in terms of the Virasoro generator $\hat{L}_0$,

$$\hat{H} = \frac{v}{R}\left(\hat{L}_0 - \frac{c}{24}\right), \qquad c = 1, \tag{3.22}$$

and it includes the Casimir energy. Furthermore, the conformal dimensions $h$, eigenvalues of $\hat{L}_0$, determine the fractional statistics $2h$ and conformal spin $h$ of excitations through the two point functions.

As shown in [12], the chemical potential $\mu$ in the expression (3.18) plays a double role: it determines the boundary conditions of the Weyl fermion on the edge, i.e. $\psi(\theta = 2\pi) = \exp(\mathrm{i}2\pi\mu)\psi(0)$, and parameterizes the following ground-state expectation values:

$$\hat{L}_n|\Omega,\mu\rangle = \hat{\rho}_n|\Omega,\mu\rangle = 0, \qquad n > 0, \tag{3.23}$$

$$\hat{L}_0|\Omega,\mu\rangle = \frac{1}{2}\left(\frac{1}{2} - \mu\right)^2 |\Omega,\mu\rangle, \tag{3.24}$$

$$\hat{\rho}_0|\Omega,\mu\rangle = \left(\frac{1}{2} - \mu\right)|\Omega,\mu\rangle. \tag{3.25}$$

These values of charge and Virasoro dimension amount to finite renormalization constants that should be added to the definitions of $\hat{L}_0$ and $\hat{\rho}_0$ in (3.18) and (3.19). The two values are related among themselves by the fulfillment of the current algebra (3.21), and can actually be computed by checking the commutation relations on the expectation values $\langle\Omega,\mu|\hat{L}_n\hat{L}_{-n}|\Omega,\mu\rangle$ and $\langle\Omega,\mu|\hat{L}_n\hat{\rho}_{-n}|\Omega,\mu\rangle$ [14].

Conformal invariance of the ground-state requires that the values in equations (3.24) and (3.25) vanish and thus the chemical potential is dynamically tuned to $\mu = 1/2$, corresponding to standard antiperiodic boundary conditions for fermions. Other values of $\mu$ are possible, but they have specific physical meaning: for example, $\mu = 0$ for periodic fermions corresponds to another (Ramond) sectors of the theory, that is non-perturbatively related to the (Neveu–Schwarz) antiperiodic sector. In the following, the values $\mu = 1/2 + \mathbb{Z}$ will also be considered for realizing features of the dynamics of edge states.

## 4. Orbital spin in the edge theory

In section 3, we saw that the effective theory predicts non-vanishing values for charge and spin at the edge of the disc, respectively proportional to the average orbital spin $\overline{s}$ and average square $\overline{s^2}$, equations (2.10) and (2.11). In this section, we are going to discuss how these effects can be realized in the microscopic description of the edge for integer fillings in section 3. These ground-state values of charge and spin follow from a kind of Casimir effect in the relativistic conformal theory, after careful discussion of the (re)normalization conditions. As a matter of fact, we show that these effects are rather non-generic in the integer Hall effect with dynamic edge excitations. On the other hand, in the case of fractional fillings discussed in section 5, we shall argue that such ground-state values should be expected.

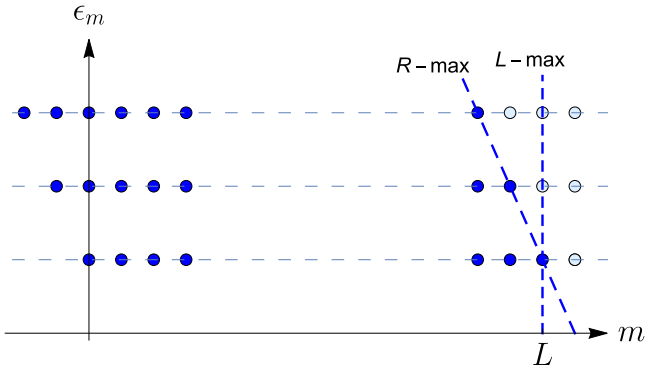


**Figure 2.** $L-\max$ versus $R-\max$ qualitative boundary conditions.

### *4.1. Qualitative boundary conditions*

In compact spatial geometries, the linear relation between Landau level degeneracy and flux is corrected by a finite amount, the so-called shift, proportional to the orbital spin $s_n$, as shown by equation (2.9). For the integer Hall effect on the sphere, the degeneracy is given by $D_n = N_\phi + 2s_n = N_\phi + 2n + 1$, where $n = 0, 1, \ldots$ is the level.

In the case of the disk, half of this correction (apart from the 1/2) can indeed be realized when the levels are filled up to a common value $L$ of angular momentum, leading to $D_n = L + n$ (see figure 2). This truncation of the spectrum, dubbed $L-\max$, can ideally be obtained by cutting the sphere in two discs. The question we want to address in the following is whether this boundary condition can be realized in a physical boundary with edge excitations.

The analysis in section 3 of wave functions with momenta $m$ near $L$, $m = L + m'$, equation (3.9), shows that they are Gaussian peaked at positions $x = (m' + n)/2R$, with $r = R + x$, $R^2 = L$. This implies that for a common value of momenta, e.g. $m' = 0$, the states of higher levels are slightly displaced outward by $\Delta x = n/R$. In presence of boundary conditions due to a confining potential or a maximum spatial extension, dubbed $R-\max$, such states acquire higher energies. Therefore, we may expect that the filling of levels up to a common Fermi energy could imply $m \leqslant L - n$, leading to equal filling $D_n = L$ for each level (see figure 2). In this case, the shift predicted by the effective action of section 2 would be washed out.

In conclusion, a 'geometric' boundary condition of the kind $L-\max$ would realize the prediction of equation (2.9), while a 'dynamic' condition of the kind $R-\max$ would give no effect. In the following, we describe the detailed realization of these two cases.

### *4.2. Edge spectrum*

The chiral conformal field theory of the Weyl fermion possesses a linear spectrum of edge excitations of the form [12]:

$$\varepsilon(k) = v(k - k_{\rm F} - \mu) = \frac{v}{R}(m' - \mu), \qquad |m'| < O(\sqrt{L}), \quad L = R^2, \tag{4.1}$$

where $k$ is the edge momentum, $v$ and $k_{\rm F}$ are the Fermi velocity and momentum, $\mu$ is the chemical potential and $m'$ the angular momentum with respect to the value $L$ near the boundary. Indeed, by inserting this spectrum in the second-quantized fermion Hamiltonian, one

reproduces the expected form $\hat{H} = v\hat{L}_0/R + \text{const.}$ (3.22) with the Virasoro generator given by (3.18).

We now discuss the confining potentials that can lead to a linear spectrum. We consider 'macroscopic' potentials of the form $V(r) \sim r^k/R^{k-1}$, with $k = 1, 2, \ldots$, that are smooth functions of the coordinate $r$ and have a linear term in the expansion near the edge $r = R + x$, $x = O(1)$ for $R \to \infty$. Upon subtracting the infinite term, the expansion near the edge takes the form:

$$V(x, R) = a_1 x + a_2 \frac{x^2}{R} + a_3 \frac{x^3}{R^2} + \cdots , \tag{4.2}$$

where the coefficients $a_i$ are dimensionless numbers (the common dimensional scale $1/\ell^2$ is implicit). Other forms of the potential polynomial in $x$ would introduce dimensional constants that break scale invariance: they correspond to non-relativistic corrections to the conformal theory that are disregarded here (see appendix A).

Furthermore, the potential should grow monotonically, because oscillations would create additional chiral-antichiral pairs of edge modes that interact and become massive, as analyzed in the studies of edge reconstruction [29]. These oscillations, expanded in the basis of Hermite polynomials $V = \sum_n b_n H_n(x)$ could single out one edge from the others, as discussed in section 3.

The determination of the energy spectrum of the Landau levels with potential (4.2) can be done analytically in the limit $R \to \infty$ and the result is the following (see appendix B). The terms $O(x^k/R^{k-1})$ with $k = 3, 4, \ldots$ in (4.2) yield subleading corrections with respect to $O(1/R)$, and one is left with a one-parameter family of potentials corresponding to the linear and quadratic terms. The corresponding spectrum is:

$$\varepsilon_{n,m'} = 2n + 1 + \frac{v}{R}\,(m' + n(2 + b)) + \text{const.}, \qquad |m'| < O(R), \tag{4.3}$$

where $n = 0, 1, \ldots$ is the Landau level index, $(2n + 1)$ is the bulk energy and the constants are related to the parameters of (4.2) by $a_1 = 2v$ and $a_2 = v(1 + b)$. In particular, $b = 0$ corresponds to the simpler quadratic potential $V = vr^2/R$.

The result (4.3) shows that in higher Landau levels the spectrum at fixed momentum $m'$ is shifted upward by an amount $O(n/R)$ as anticipated by the qualitative argument at the beginning of this chapter. This is the effect of the orbital spin at the edge, more precisely of the differences $s_n - s_{n-1} = n$ between levels, because a constant term can be added at will. This result is not completely universal, i.e. independent of the form of boundary potentials compatible with scale invariance at the edge, since it involves one free parameter $b$, corresponding to the quadratic correction to linearization.

In conclusion, the microscopic Hamiltonian of the $\nu = n$ Hall effect with boundary potential takes the form:

$$\begin{aligned} \hat{H} &= \hat{H}_0 + \frac{v}{R} \int \mathrm{d}z^2 \hat{\Psi}^\dagger\, V(x, R)\, \hat{\Psi} + \text{const.} \\ &= \sum_{i=0}^{n} \sum_{m_i \in \mathbb{Z}} \left[ 2i + \frac{v}{R}\,(m_i + s_i(2 + b) - \alpha) \right] \hat{d}^{(i)\dagger}_{m_i} \hat{d}^{(i)}_{m_i} + \text{const.}. \end{aligned} \tag{4.4}$$

In this equation, $\hat{H}_0$ is the bulk Hamiltonian (3.1), the momenta $m_i$ are measured w.r.t. $L = R^2$ and the constant term $\alpha$ is put explicitly.

The correction to the linear edge dispersion relations (4.4) due to the shifts $s_i$ is rather relevant for the following discussion. We remark that this effect cannot be modified, apart from

the overall constant $\alpha$. Moreover, in the geometry of the annulus, the antichiral edge modes of the inner circle possess the same spectrum (4.4) with $v \to |v|$ and same shifts.

### 4.3. Map to conformal field theory

We now identify the edge Hamiltonian (4.4) with the conformal theory form (3.18), i.e. compare the following two expressions level by level,

$$\hat{H}^{(i)} = \frac{v}{R}\sum_{m_i\in\mathbb{Z}}\left[2i + \frac{v}{R}\left(m_i + \frac{(2i+1)(2+b)}{2} - \alpha\right)\right]\hat{d}^{(i)\dagger}_{m_i}\hat{d}^{(i)}_{m_i}, \tag{4.5}$$

$$\frac{v}{R}\hat{L}^{(i)}_0 = \frac{v}{R}\sum_{k_i\in\mathbb{Z}}(k_i-\mu_i) : \hat{d}^{(i)\dagger}_{k_i}\hat{d}^{(i)}_{k_i} :, \qquad i = 0, 1, \ldots. \tag{4.6}$$

Note that the conformal Hamiltonian does not include the bulk energy, that is assumed to be constant for edge physics, because bulk-boundary electron transitions are disregarded. The conformal description is robust to deformations that set independent Fermi velocities for each level, $v \to v_i$, being non-universal parameters; in the following, we keep a single velocity without loss of generality.

This matching of the two Hamiltonians (4.5) and (4.6) involves two aspects:

- The $2s_i = 2i + 1$ shift in the dispersion relation can be accounted for by assuming level-dependent values for the chemical potential $\mu_i$ in the conformal theory description of the $i$th level. This setting leads to physically observable effects of the orbital spin.
- The conformal mode index $k_i$ in (4.6) can also be translated w.r.t. the edge momentum $m_i$, in order to match the actual filling of the $i$th Landau level with the conformal vacuum (3.20), conventionally filled up to level $k_i = 0$.

Let us first identify the conformal theory for the lowest Landau level, $i = 0$. For $N = L + 1$ electrons, the ground-state is filled up to level $m = L$, thus the conformal moding and edge momentum precisely match, $k_0 = m_0$. The conformal invariant value $\mu = 1/2$ for the chemical potential is fixed by adjusting the constant $\alpha$ of the confining potential (4.4), as follows:

$$\mu_0 = \frac{1}{2}, \qquad \alpha = \frac{3}{2}, \qquad (k_0 = m_0)\,. \tag{4.7}$$

The determination of the conformal theories for higher levels depends on the physical setting. We can distinguish two cases, that are analyzed in the following paragraphs.

*4.3.1. Smooth boundary.* Let us consider the filling of the first two Landau levels up to a common Fermi energy, in presence of the boundary potential (4.2) (see figure 3). The comparison of energies (4.3), $\varepsilon_{0,m_0} = \varepsilon_{1,m_1}$, gives:

$$m_0 = \frac{2R}{v} + m_1 + 2 + b. \tag{4.8}$$

Being $m_0 = 0$ for the lowest-level ground-state, this equation shows that the second edge branch is located around momenta $m_1 \sim -2R/v$. Therefore, the corresponding conformal theory should be defined with respect to shifted momenta, as follows:

$$k_1 = m_1 - 2R/v - 2 - b, \qquad \mu_1 = \frac{1}{2}. \tag{4.9}$$

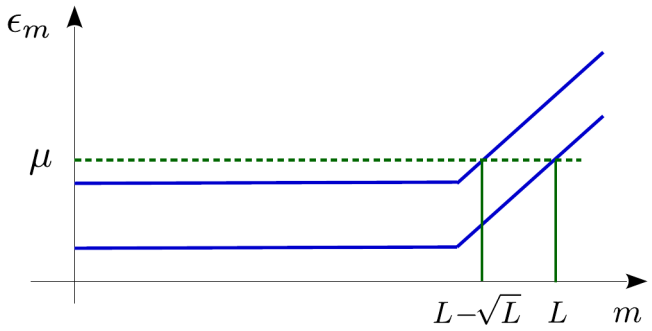


**Figure 3.** Filling of two Landau level according to the spectrum (4.3).

Recalling that $R = \sqrt{L}$ is large, this can be adjusted by $O(1)$ corrections such that the difference $k_1 - m_1$ is an integer and independent of $s_1$, in particular. The chemical potential $\mu_1$ is again fixed by requiring vanishing ground-state charge and conformal spin.

This is the realization of the $R-\max$ boundary condition described at the beginning of this section: the effect of the shift is cancelled because the conformal field theories of the two edge branches are defined independently one of the other. Note that the relative wavefunctions are at distance $\Delta m \sim 2R$, i.e. $\Delta x \sim 21$ and thus have exponentially small overlaps. There are no particle exchanges between the two edges in agreement with the independent conservation of the relative charges.

In conclusion, for isolated droplets with smooth confining potentials the edge excitations of different levels are orthogonal and the system realizes the $R-\max$ qualitative boundary setting, leading to no orbital spin effects. We have verified that the same behavior is present in the Landau level spectrum with Dirichlet boundary conditions at $r = R$. Finally, when the system is connected to an electron reservoir, the edge branches are let to interact, but their chemical potentials level off and there is no effect either.

*4.3.2. Sharp boundary.* We now discuss the realization of the $L-\max$ sharp boundary condition introduced at the beginning of this section. We must assume that the bulk energy of Landau levels in (4.3) is absent; this could be due to the bulk interactions of electrons in the incompressible fluid, that were not included in the previous microscopic theory. For example, there could be a level-dependent screening of the Coulomb interaction, but we have no proof of this fact. Let us nonetheless analyze the map to conformal field theory in this setting.

The dispersion relations $\varepsilon_{n.m}$ for vanishing bulk term show that the different branches of edges occur in the same $O(1/R)$ range of energies and for close momenta $m_i$ values, such that the corresponding wavefunctions do overlap. The $n$ branches are now parts of the same $c = n$ conformal theory and it necessary to define a unique ground-state with a common definition of edge momentum. This is given by:

$$k_i = m_i = m_0, \qquad i = 1, 2, \ldots, \tag{4.10}$$

such that all levels are filled up to $m_i = 0$. This ground-state is translation invariant for all the levels; otherwise said, there are no persistent currents at the edge.

The matching of microscopic and conformal Hamiltonians (4.5) and (4.6) is achieved in this case by allowing a different chemical potential for each level (we set $b = 0$ momentarily):

$$\mu_i = \frac{1}{2} - 2i, \qquad i = 1, \ldots, n-1. \tag{4.11}$$

These values of $\mu_i$ imply that the higher Landau levels possess non-vanishing ground-state values of charge and conformal spin (dimension), as described in section 3, equations (3.24) and (3.25):

$$\hat{\rho}_0^{(i)}|\Omega,\mu_i\rangle = 2i\,|\Omega,\mu_i\rangle, \qquad \mu_i = \frac{1}{2} - 2i, \tag{4.12}$$

$$\hat{L}_0^{(i)}|\Omega,\mu_i\rangle = 2i^2\,|\Omega,\mu_i\rangle. \tag{4.13}$$

It turns out that these states are actually excitations with respect of the standard vacuum with $\mu = 1/2$. This realization of the $L-\max$ boundary condition is shown in figure 4(b) next to the earlier $R-\max$ condition in figure 4(a).

The total ground-state charge and conformal spin for $\nu = n$ are given by the sum of the contributions of all the levels:

$$\begin{aligned} Q_{\rm b} &= \sum_{i=0}^{n-1} 2i = n(n-1), \\ \mathcal{S}_{\rm b} &= \sum_{i=0}^{n-1} 2i^2 = \frac{n(n-1)(2n-1)}{3}. \end{aligned} \tag{4.14}$$

These also imply the ground-state energy:

$$E_{\rm b} = \frac{v}{R}\left(\mathcal{S}_{\rm b} - \frac{c}{24}\right), \qquad c = n. \tag{4.15}$$

This is the anticipated Casimir effect due to the orbital spin.

Let us add some remarks:

- The ground-state values (4.12) and (4.13) acquire factors, respectively, $(1 + b/2)$ and $(1 + b/2)^2$ for general quadratic terms in the confining potential (4.2). Thus the Casimir effect is not fully universal.
- However, the allowed values of the chemical potential are $\mu_i = 1/2 + \mathbb{Z}$, corresponding to antiperiodic boundary conditions for fermions; real values of $\mu_i$ would cause unphysical non-analyticities in electron correlators. In other words, the charge accumulated in the ground-state $Q_{\rm b}$ should be an integer. This implies that only $b \in \mathbb{Z}$ is compatible with conformal invariance at the edge. A mechanism for self-tuning of $b$ is the quadrupole deformation of the droplet discussed in section 6.
- The ground-state values (4.12) and (4.13) agree with the effective field theory results (2.11) and (2.10) for the special case $b = -1$.

In conclusion, we have found that the edge effects parameterized by the orbital spin can indeed been found in the microscopic description when a unique conformal theory encompasses all edges branches. This definition of edge theory is non-generic in the case of the integer Hall effect, where separate branches are possible, but it is necessary for describing interacting edges, such as those of the hierarchical Jain states discussed in the next section.

## 5. $W_\infty$ symmetry and fractional fillings

In this section, the edge theory with integer fillings is rederived by using the symmetry of incompressible Hall fluids under area-preserving diffeomorphisms of the plane, the $W_\infty$ symmetry [22–24]. This reformulation allows us to extend our analysis to fractional fillings and

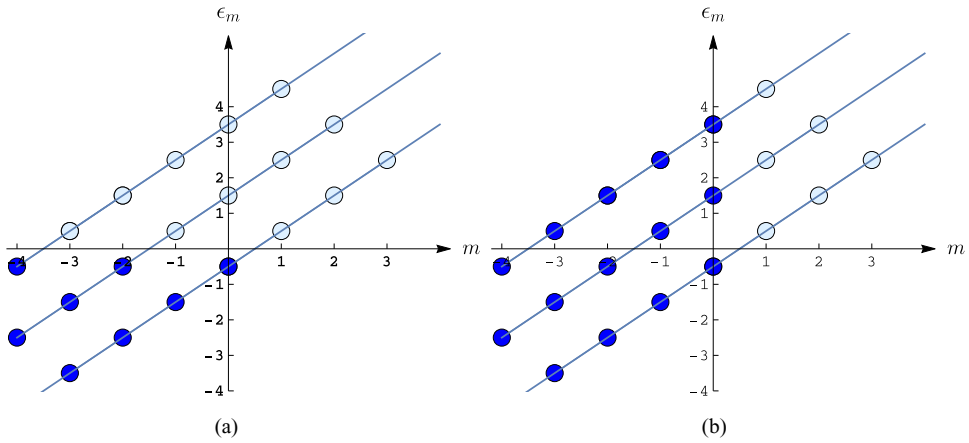


**Figure 4.** Fock space near the Fermi surface of the $\nu = 3$ droplet in two different setups: (a) all levels with same chemical potential, $\mu_i = 1/2$, corresponding to vanishing ground-state energy; (b) all levels filled up to the same momentum $m_i = 0$.

in particular to hierarchical states, which also possess several branches of edge modes and corresponding $s_i$ values.

### *5.1. Edge excitations as $W_\infty$ transformations*

We consider the filled lowest Landau level as a starting point of our discussion. As is well known, the electrons form a droplet of incompressible fluid that is characterized by constant density and constant area $\mathcal{A}$. The deformations of the fluid at energies below the bulk gap can be generated by coordinate transformations of the plane that keep the density constant in the bulk. These corresponds to the area-preserving diffeomorphisms that modify the shape of the droplet at fixed area [22–24].

At the classical level, these reparameterizations are expressed in terms of a scalar generating function $w(z, \bar{z})$ and Poisson brackets. Their action on the coordinate and the density $\rho$ is given by the following expressions:

$$\delta_\omega z = \{z, w\} = \varepsilon^{z\bar{z}} \partial_z z \partial_{\bar{z}} w + (z \leftrightarrow \bar{z}), \qquad \delta_w \rho = \{\rho, w\}, \tag{5.1}$$

where $\varepsilon^{z\bar{z}} = -\varepsilon^{\bar{z}z} = -2\mathrm{i}$. In the geometry of the disk, the ground-state density is constant in the bulk and goes to zero at the boundary: the deformation by Poisson brackets (5.1) involves the derivative of the density that has support on the boundary, as expected.

At the quantum level, the quantities in (5.1) become one-body operators,

$$\hat{\rho} = \hat{\Psi}^\dagger \hat{\Psi}, \qquad \hat{w} = \int \mathrm{d}^2 z \hat{\Psi}^\dagger(z, \bar{z}) w(z, \bar{z}) \hat{\Psi}(z, \bar{z}), \tag{5.2}$$

involving the field operator $\hat{\Psi}$ restricted to the first Landau level. The Poisson brackets (5.1) are replaced by commutators, $\delta\hat{\rho} = \mathrm{i}\,[\hat{\rho}, \hat{w}]$. The ground-state expectation value gives the transformation of the density function, that takes the following form [10, 24]:

$$\delta\rho\,(z, \bar{z}) = \langle\Omega|\,[\hat{\rho}(z, \bar{z}), \hat{w}]\,|\Omega\rangle = \mathrm{i} \sum_{n=1}^{\infty} \frac{(2\hbar)^n}{B^n n!} \left(\partial_{\bar{z}}^n \rho \partial_z^n w - \partial_z^n \rho \partial_{\bar{z}}^n w\right) = \{\rho, w\}_{\mathrm{M}}\,. \tag{5.3}$$

This formula defines the Moyal brackets $\{\rho, w\}_{\mathrm{M}}$, that are non-local due to the non-commutativity of coordinates in the lowest Landau level. There appears an expansion in $\hbar/B$, whose first term reproduces the classical transformation law (5.1).

Equation (5.3) expresses the $W_\infty$ transformations of the density at the quantum level. Another formulation of this symmetry involves the Girvin–MacDonald–Platzman sin-algebra [30], that corresponds to the commutator of two densities in Fourier space: similar to equation (5.3), this algebra is given by the Moyal brackets of the classical densities.

In the following, we discuss the form of the leading $O(1/B)$ term in the Moyal brackets, while the higher orders $O(1/B^k)$ will be briefly discussed in appendix A. The density $\rho^{(0)}$ of the filled lowest level in the disk geometry is a function of the radius only, $\rho^{(0)} = \rho^{(0)}(r)$. Thus, the leading $W_\infty$ deformation of the ground-state can be written as follows:

$$\delta\rho^{(0)}(r,\theta) = \frac{2\mathrm{i}}{B}\,\bar\partial\rho^{(0)}\,\partial w + h.c. = \frac{1}{rB}\left(\partial_r\rho^{(0)}(r)\right)\partial_\theta w(r,\theta). \tag{5.4}$$

We now define the Fourier modes of the edge density by integrating in space the bulk density, following the same steps of the analysis in section 3,

$$\delta\rho_k^{(0)} = \int \mathrm{d}\theta\,\mathrm{e}^{-\mathrm{i}k\theta}\int \mathrm{d}r r\,\delta\rho^{(0)}. \tag{5.5}$$

It is also convenient to expand the generating function in Fourier modes, leading to ($B = 2$ hereafter):

$$\delta\rho_k^{(0)} = \frac{\mathrm{i}k}{2}\int \mathrm{d}r\left(\partial_r\rho^{(0)}(r)\right)w_k(r), \qquad w(r,\theta) = \frac{1}{2\pi}\sum_{n\in\mathbb{Z}} w_n(r)\,\mathrm{e}^{\mathrm{i}n\theta}. \tag{5.6}$$

The remaining integral over the radial dependence is non-vanishing in a shell $r = R \pm O(1)$, as understood in section 3. In order to compute the integral, we can use the exact expression for the derivative of the density of filled Landau levels derived in [28]. For the $i$th level filled with $N$ electrons, it reads:

$$\frac{\mathrm{d}}{\mathrm{d}r^2}\rho^{(i)}(r) = -i!\,\frac{\mathrm{e}^{-r^2}r^{2N-2\mathrm{i}-2}}{(N-1)!}L_i^{N-i-1}(r^2)\,L_i^{N-i}(r^2). \tag{5.7}$$

The expression for the lowest level is evaluated in the limit to the edge defined in section 3, finding the result,

$$\partial_r\rho^{(0)}(R+x) \simeq -2\mathrm{e}^{-2x^2}, \qquad R\to\infty, \quad x = O(1). \tag{5.8}$$

Thus, it is again useful to use Hermite polynomials $H_{2n}(2x)$ for analyzing the radial dependence of edge excitations. We obtain:

$$\delta\rho_k^{(0)} = -\mathrm{i}k\,w_{0k}, \qquad w(r,\theta) = \frac{1}{2\pi}\sum_{n\in\mathbb{Z}}\sum_{i=0}^{\infty} w_{ik}\,H_{2i}(\sqrt{2}x)\,\mathrm{e}^{\mathrm{i}n\theta}. \tag{5.9}$$

This classical amplitude of fluctuations should be compared with the simplest excitation of the $c = 1$ conformal theory, that is given by the current-algebra mode applied to the ground state, $|ex\rangle \sim \hat\rho_{-m}^{\mathrm{CFT}}|\Omega\rangle$. Therefore, the conformal theory analog of the $W_\infty$ density fluctuation (5.9) reads,

$$\delta\rho_k^{\mathrm{CFT}} = \mathrm{i}\langle\Omega|\left[\hat\rho_k^{\mathrm{CFT}}, \hat\rho_{-m}^{\mathrm{CFT}}\right]|\Omega\rangle = \mathrm{i}\delta_{km}k. \tag{5.10}$$

The equivalence of the results (5.9) and (5.10) directly shows the relation between the bulk $W_\infty$ symmetry and the edge conformal symmetry.

The $W_\infty$ deformations in higher filled levels are described in similar fashion. The transformations act horizontally within each level [22], that can be analyzed independently; this matches the fact already discussed that the corresponding branches of edge excitations are orthogonal. The fluctuations of the second level are given by:

$$\delta\rho^{(1)} = \mathrm{i}\langle\Omega^{(1)}|\left[\hat{\rho}^{(1)}, \hat{w}^{(1)}\right]|\Omega^{(1)}\rangle, \tag{5.11}$$

where $\hat{\rho}^{(1)} = \hat{\Psi}^{(1)\dagger}\hat{\Psi}^{(1)}$ is the corresponding density operator, and the generator is expressed as:

$$\hat{w}^{(1)} = \int \mathrm{d}^2 z\, \hat{\Psi}^{(1)\dagger} w\,(z,\bar{z})\, \hat{\Psi}^{(1)}, \tag{5.12}$$

in terms of the field operator $\hat{\Psi}^{(1)}$ restricted to the second level. We now remark that expressions like (5.11) and (5.12) can be mapped into lowest level formulas by using the relations among wavefunctions (3.3), such as $\psi_{1,m} = a^\dagger \psi_{0,m+1}$. This corresponds to a differential relation between the field operators of the two levels, leading to:

$$\hat{\rho}^{(1)} = \left(1 + \partial\bar{\partial}\right)\hat{\rho}^{(0)}, \tag{5.13}$$

and

$$\hat{w}^{(1)} = \int \mathrm{d}^2 z\, \hat{\Psi}^{(0)\dagger}\left[\left(1 + \partial\bar{\partial}\right) w\right]\hat{\Psi}^{(0)}, \tag{5.14}$$

implicitly assuming the isomorphism of the two Fock spaces. The corresponding relations among classical functions are:

$$\rho^{(1)} = \left(1 + \partial\bar{\partial}\right)\rho^{(0)}, \qquad w^{(1)} = \left(1 + \partial\bar{\partial}\right) w. \tag{5.15}$$

These differential relations map the second level density fluctuations (5.11) into expressions that are defined on the first level, for which the Moyal brackets (5.3) apply. Moreover, the two kinds of differential relations commute. Therefore, the leading $O(1/B)$ second level fluctuations are of the same form (5.4):

$$\delta\rho^{(1)} = \frac{1}{rB}\partial_r\rho^{(1)}\ \partial_\theta w^{(1)}. \tag{5.16}$$

The edge moments are again defined by Fourier analysis in $\theta$ and radial integration as in equations (3.12) and (5.5). For the derivative of the density we can consider the $R \to \infty$ limit of the exact formula (5.7) or use the differential relation (5.13), leading to $\partial_r\rho^{(1)} = \partial_r(1 + \partial\bar{\partial})\rho^{(0)} \simeq -8x^2\mathrm{e}^{-2x^2}$. Using this result together with (5.16) and (5.5), we obtain:

$$\delta\rho_k^{(1)} \simeq -\mathrm{i}k \int \mathrm{d}x\, 8x^2\mathrm{e}^{-2x^2}\left(1 + \partial\bar{\partial}\right)\sum_{i=0}^{\infty} w_{ik}\, H_{2i}(\sqrt{2}x). \tag{5.17}$$

This fluctuations involve contributions from the first three radial moments $(w_{0k}, w_{1k}, w_{2k})$. In the same way as the conformal field theory (operator) description of section 3, the edge excitations of higher levels are associated to higher radial moments of the bulk density evaluated in the region $r = R + x$, with $x = O(1)$.

The analysis can be extended to the third Landau level: by using the relation between wavefunctions, we can again establish a differential map to the first level:

$$\hat{\rho}^{(2)} = \left[1 + 2\partial\bar{\partial} + \frac{1}{2}\left(\partial\bar{\partial}\right)^2\right]\hat{\rho}^{(0)}. \tag{5.18}$$

Together with the analogous one for the generator $\hat{w}^{(2)}$, one can compute the $W_\infty$ deformations of the ground-state density (5.3) whose radial moments involve further terms of the radial expansion in Hermite polynomials.

The combination of the previous results finally yield the edge excitations for integer filling fraction obtained from the $W_\infty$ transformations of incompressible ground-states. For example, in the $\nu = 2$ case, we find using (5.9) and (5.17):

$$\delta\rho_k^{(\nu=2)} = \delta\rho_k^{(0)} + \delta\rho_k^{(1)} = -\mathrm{i}k\left(a_0 w_{0k} + a_1 w_{1k} + a_2 w_{2k}\right), \tag{5.19}$$

where $(a_0, a_1, a_2)$ are numerical coefficients that parameterize the radial dependence at the edge.

In conclusion, in this section we have shown that the $W_\infty$ transformations of the ground-state for integer fillings $\nu = n$ generate edge excitations that match the conformal field theory description of section 3: in particular, the $n$ independent branches of excitations are associated to different radial moments of the density in a finite shell at the boundary, $r - R = O(1)$. As discussed in section 3, equation (3.17), it is possible to single out one particular component by integrating the density with specific radial weights and using the orthogonality of Hermite polynomials.

### 5.2. Edge excitations and orbital spin for fractional fillings

The $W_\infty$ description of edge excitations is particularly useful because it holds for any incompressible fluid ground-state, including fractional fillings. Namely, the Moyal brackets (5.3) correctly give the low-energy excitations that can be divided in several branches by studying the radial moments of the density. In summary, this approach provides the general and universal kinematics of edge excitations. In the integer filling case, it shows that the description of edge states remains valid when bulk interactions are introduced that preserve incompressibility, i.e. do not close the gap. Furthermore, this approach extends directly to the fractional Hall effect and provides a unique derivation of the edge conformal field theory.

The difference between the integer and fractional filling lies in the energetics of excitations, i.e. in the form of the edge Hamiltonian. In the integer case, a direct microscopic derivation was possible as shown in section 4. For fractional states, the edge dynamics is due to the many-body interactions and cannot be derived analytically. The standard approach, based on the effective action of section 2 and bosonization of the edge fermions predicts that the Hamiltonian takes the Luttinger current–current form [14],

$$\hat{H} = \sum_i \frac{v^{(i)}}{R}\left(\hat{L}_0^{(i)} - \frac{1}{24}\right), \qquad \hat{L}_0^{(i)} = \sum_{k\in\mathbb{Z}} :\hat{\rho}_{-k}^{(i)}\hat{\rho}_k^{(i)}: \ . \tag{5.20}$$

This conformal theory still possesses integer central charge and the spectra of charges and conformal spins are given by the weight lattice with Gram matrix $K^{-1}_{(i)(j)}$ in equation (2.4) as follows:

$$Q_{\mathrm{b}} = \lambda^T K^{-1} t, \qquad \mathcal{S}_{\mathrm{b}} = \frac{1}{2}\lambda^T K^{-1}\lambda, \qquad \lambda = (\lambda_1, \ldots, \lambda_n), \quad \lambda_i \in \mathbb{Z}, \tag{5.21}$$

where $t = (1, 1, \ldots, 1)$ is the so-called charge vector and $\lambda_i$ characterize the excitations.

Although this theory has not been completely proven, analytic and numerical results confirm its predictions, such as that the Laughlin states with $\nu = 1/(q+1)$, with $q$ even, possesses a single branch, while the hierarchical Jain states with $\nu = n/(qn+1)$ show $n$ branches. The extensive phenomenology based on the composite fermion correspondence [31] between integer and hierarchical states let us argue that the structure of branches found for integer fillings also describe the Jain states.

Regarding the role of the orbital spins $s_i$, we cannot prove that the analysis of section 4 extends to Jain states, having no direct derivation of their effect on the energy spectrum. Nonetheless, based on some reasonable assumptions, we present a self-consistent argument for the existence of ground-state values of charge and spin in the edge theory as predicted by the effective theory of section 2.

Since the hierarchical states are interacting, their conformal theory should be built around a single ground-state, imposing the $L - \max$ boundary conditions of figure 4(b). As discussed in section 4.3.2, the resulting ground-state is actually an excited state from the conformal theory point of view, corresponding to a number of electrons added to the standard conformal vacuum $|\Omega\rangle_{\rm CFT}$, obeying:

$$\rho_0|\Omega\rangle_{\rm CFT} = L_0|\Omega\rangle_{\rm CFT} = 0. \tag{5.22}$$

Such ground-state $|\Omega, k, h_k\rangle$ with charge $Q_{\rm b} = k \in \mathbb{Z}$ and conformal spin $\mathcal{S}_{\rm b} = h_k$ has the form:

$$\begin{aligned} |\Omega, k, h_k\rangle &= \lim_{\tau_k \to -\infty, \tau_1 > \tau_2 > \cdots > \tau_k} : V_e(\eta_k) \cdots V_e(\eta_1) : |\Omega\rangle_{\rm CFT} \\ &= \lim_{\eta \to 0} V_{ke}(\eta)|\Omega\rangle_{\rm CFT}. \end{aligned} \tag{5.23}$$

In this expression, $\eta_j = \exp((\tau_j + {\rm i}R\theta_j)/R)$, where $\tau_j + {\rm i}R\theta_j$ are the coordinates of the edge spacetime cylinder and $V_e(\eta)$ is the vertex operator for the electron field on the edge; the normal-ordering $(: :)$ should be evaluated by fusing $k$ electrons in the conformal theory, leading to the $Q_{\rm b} = k$ field $V_{ke}$. Since electrons have integer mutual statistics w.r.t. all the excitations of the theory, the insertion of these fields at infinity does not cause additional nonlocalities in edge correlation functions, that are actually independent of the insertion points $\eta_j$.

Let us assume that this ground-state is realized and run the consistency check. We first determine the orbital spins $s_i$ for the hierarchical states. In the multicomponent Wen–Zee action of section 2, the parameters $\nu$, $\nu\bar{s}$ and $\nu\overline{s^2}$ are given by the general expressions (2.4):

$$\nu = t^T K^{-1} t, \qquad \nu\bar{s} = t^T K^{-1} s, \qquad \nu\overline{s^2} = s^T K^{-1} s, \tag{5.24}$$

upon inserting the $s = (s_0, s_1, \ldots, s_{n-1})$ vector and the matrix $K = I + qC$, where $C$ is the $n \times n$ matrix with all entries equal to one. One finds:

$$\nu = \frac{n}{nq+1}, \qquad \nu\bar{s} = \frac{1}{nq+1}\sum_i s_i = \frac{n}{nq+1}\frac{q+n}{2}, \tag{5.25}$$

with $n = 1, 2, \ldots$ and $q = 0, 2, 4, \ldots$. In the second equation, we also wrote the value $\bar{s} = (q+n)/2$ obtained from the angular momentum of the Jain wavefunctions [31] and equation (2.5). The relation (5.25) identifies the following values:

$$s_i = \left(\frac{q+1}{2}, \frac{q+3}{2}, \ldots, \frac{q+2n-1}{2}\right). \tag{5.26}$$

Namely, they take half-integer values and their differences are integer, as expected.

The comparison of these bulk data with the edge conformal theory involves two steps: (i) the ground-state charge $Q_\mathrm{b}$ and spin $\mathcal{S}_\mathrm{b}$ should correspond to electron excitations of the edge theory; (ii) they should be parameterized by integers $\lambda_i$ that are equal to the orbital spin values (5.26) up to a constant, $\lambda_i = s_i + \Delta$.

Let us verify that these two conditions can be met. The electron excitations have the spectrum:

$$Q_\mathrm{b} = \Lambda^T t, \qquad \mathcal{S}_\mathrm{b} = \frac{1}{2}\Lambda^T K \Lambda, \qquad \Lambda = (\Lambda_1, \ldots, \Lambda_n), \quad \Lambda_i \in \mathbb{Z}, \tag{5.27}$$

corresponding to the integer-charge subset of the general excitation spectrum (5.21), i.e. $\lambda = K\Lambda$.

Note the similarity between the expressions (5.21) for (fractional) charged excitations and those involving the $s_i$ (5.24) that we want to reproduce. Since the orbital spin values differ by integers, $s_{i+1} - s_i = 1$, we seek for solutions $\lambda_i$ with the same property $\lambda_{i+1} - \lambda_i = 1$. Upon inspection, we find that they do exist and are given by:

$$\lambda_i = \Lambda_i + q\sum_j \Lambda_j, \qquad \Lambda_i = (0, 1, 2, \ldots, n-1), \tag{5.28}$$

correctly obeying $\lambda_i = s_i + \Delta$. Actually, these electron excitations are possible due to the particular form of the matrix $K$ of hierarchical states.

The ground-state values of charge and spin are finally given by:

$$Q_\mathrm{b} = \sum_i \Lambda_i = \frac{n(n-1)}{2}, \qquad \nu = \frac{n}{nq+1},$$
$$\mathcal{S}_\mathrm{b} = \frac{n(n-1)(2n-1)}{12} + \frac{q}{2}\left(\frac{n(n-1)}{2})\right)^2. \tag{5.29}$$

Note that the value of the integer charge is the same as in the $\nu = n$ case (4.14) (for parameter $b = -1$).

In conclusion, we have found the expressions of the orbital spins $s_i$ of hierarchical states (5.26) and shown that their values shifted by a common constant correctly parameterize ground-state charge and conformal spin in the edge theory.

## 6. Signatures of the orbital spin at the edge

A thorough discussion of the experimental setups that may led to the observation of the orbital spin $s_i$ in edge physics is beyond the scope of this work. In the following, we sketch two possible settings where an effect could be seen, at least in principle. We discuss the isolated Hall droplet (no conduction) with sharp boundary conditions, discussed in section 4.3.2, that can be realized with small droplets.

### *6.1. Coulomb blockade*

In the experiment of Coulomb blockade, an electron tunnels into an isolated droplet at zero bias. As discussed in [25], the energy of charged edge states can be continuously deformed by changing the capacity of the droplet, i.e. by squeezing its area. The energy of the $k$-electron excitation over the ground-state, as given by the eigenvalue of the Virasoro operator $L_0$, is modified by the charging energy as follows:

$$E_k = \frac{v}{R}\frac{(k-\sigma)^2}{2}, \qquad \nu = 1, \tag{6.1}$$

where $\sigma$ is the change of flux quanta due to the squeezing of the area. When $\sigma = 1/2$, the energies of the ground and one-electron states become degenerate, $E_0 = E_1$, and an electron can tunnel inside the droplet at zero bias, causing a peak in the conductance, i.e. $\Delta Q = 1$. Successive peaks are found when $\sigma$ passes the values $1/2 + j$, for $j = 1, 2, \ldots$.

In the case of the isolated droplet with sharp boundary discussed in section 4.3.2, the electrons of the $i$th level possess higher activation energies for larger $i$ values, owing to the different chemical potentials. The previous equation is modified into:

$$E_k^{(i)} = \frac{v}{R}\left[\frac{(k-\sigma)^2}{2} + 2i(k-\sigma)\right] = \frac{v}{2R}\left[(k-\sigma+2i)^2 - 4i^2\right], \qquad i = 0, \ldots, n-1. \tag{6.2}$$

This equation shows that for the $i$th level, the first degeneracy point $E_0^{(i)} = E_1^{(i)}$ occurs at the value $\sigma = 1/2 + 2i$, while the following ones repeat at the same distance $\Delta\sigma = 1$. Namely, the different branches of edge states enter into play at different $\sigma$ values, owing to the different activation energies.

In conclusion, a possible signature of the orbital spin could be seen at the beginning of the deformation, i.e. for small $\sigma$ values. The sequence of electron tunnelings would be, for $\nu = n$,

$$\Delta Q = 1, 1, 2, 2, 3, 3, \ldots, n, n, n, \ldots, \quad \text{for} \quad \sigma + \frac{1}{2} = 1, 2, \ldots, 2n, 2n+1, 2n+2 \ldots, \qquad (\nu = n), \tag{6.3}$$

leading to a triangular comb plot for $\Delta Q(\sigma)$ (see figure 5).

### 6.2. Quadrupole deformation

Another test of the orbital spin at the edge is made by deforming the shape of the droplet. This is suggested by the effective action, because the boundary terms (2.7) couple $\bar{s}$ and $\overline{s^2}$ to the extrinsic curvature $K$, that measures shape deformations[3]

Let us consider a quadrupole deformation of the confining potential [26],

$$H \;\to\; H + V_\varepsilon = H + \frac{\varepsilon}{R}\left(z^2 + \bar{z}^2\right), \tag{6.4}$$

where $\varepsilon \ll 1$. We analyze this effect to first perturbative order in $\varepsilon$. Let us go back to the discussion of the confining potential before the limit to the edge, in appendix B. The unperturbed states $|i, m\rangle$ have energy $E_m^{(i)} = (v/R)(m + 2\mathrm{i} + 1)$, where $i$ and $m$ are level index and momentum. In the case of $\nu = n$, this unperturbed spectrum is $n$-times degenerate for given value of $k = m + 2\mathrm{i}$. The expectation value of $V_\varepsilon$ in this degenerate subspace form a $(n \times n)$ matrix whose eigenvalues give the the leading perturbative correction to the energy. The matrix is:

$$\begin{aligned}(V_\varepsilon)_{ik,jk} &= \frac{\varepsilon}{R}\langle i, m|2b^\dagger a + 2ba^\dagger|j, \ell\rangle|_{m+2\mathrm{i}=\ell+2j=k} \\ &= \frac{2\varepsilon}{R}\left(\sqrt{(i+1)(k-i)}\,\delta_{i,j-1} + \sqrt{i(k-i+1)}\,\delta_{i,j+1}\right), \\ &i, j = 0, \ldots, n-1.\end{aligned} \tag{6.5}$$

[3] We thank Wiegmann for suggesting this possibility to us.

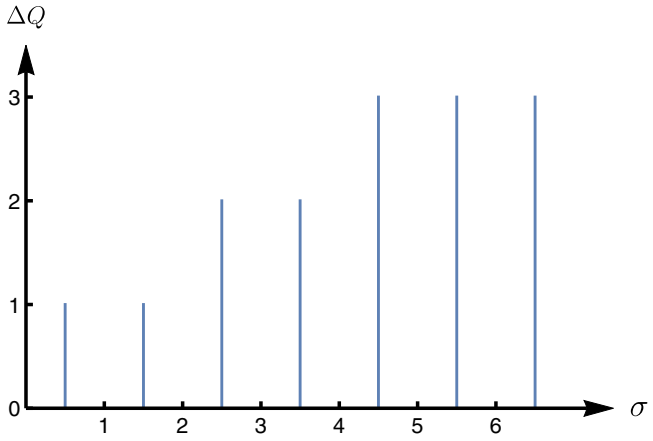


**Figure 5.** Peaks of tunneling electrons obtained by varying the number of flux quanta $\sigma$ (area) of an isolated droplet with $\nu = 3$ (see equation (6.3)).

The eigenvalues of this matrix are e.g. $(\pm 2\varepsilon\sqrt{k}/R)$ for two Landau levels and $(0, \pm 2\varepsilon\sqrt{3k-2}/R)$ for $\nu = 3$, et cetera.

Following the discussion of section 4, we should evaluate this correction in the edge limit, given by $R \to \infty$ with $r = R + x$ and $k = m + 2\mathrm{i} = R^2 + m' + 2\mathrm{i}$. We can thus approximate $k - i$ with $R^2$ in the matrix elements (6.5), simplifying the eigenvalue problem. We then find the following modification of the edge spectrum (4.3) (for $b = 0$):

$$v\langle j, L + m'|2x + \varepsilon\cos 2\theta|j, L + m'\rangle = \frac{v}{R}\left(m' + 2j + 1 + 2\varepsilon\alpha_j\right). \tag{6.6}$$

In this equation, $j = 0, \ldots, n-1$ is the index of the Landau levels (now mixed among themselves by the perturbation) and $\alpha_j$ are $O(1)$ constants, whose first few values are:

| $n$ | 2 | 3 | 4 | ... |
|---|---|---|---|---|
| $\alpha_j$ | $\pm 1$ | $0, \pm\sqrt{3}$ | $\pm\sqrt{3 \pm \sqrt{6}}$ | ... |

(6.7)

In conclusion, the quadrupole perturbation amounts, in the edge limit, to rigid $O(1/R)$ translations of the branches of the edge spectrum among themselves. Upon tuning $\varepsilon$, one can exactly compensate the translation due to the shift, e.g. by setting $2j + 2\varepsilon\alpha_j = 0$ for a given value of $j$ in (6.6). This result is consistent with the mentioned coupling of the orbital spin to the extrinsic curvature.

One physical application of the quadrupole perturbation of the Hall droplet could be the following. In the Coulomb blockade setting, a small non-integer shift among the levels could be useful to split the degeneracy of the peaks. For example, let us consider the value of $\sigma$ at which two pairs of levels become degenerate, belonging to two branches of edge states, causing a $\Delta Q = 2$ peak (see figure 5). In presence of the quadrupole deformation, this double peak splits in two $\Delta Q = 1$ peaks, occurring at slightly different values of $\sigma$. The same pattern repeats itself at distance $\Delta\sigma = 1$. This fact could help interpreting the experimental results.

## 7. Conclusions

In this work we explicitly found the structure of edge excitations in the multicomponent case, and showed that the various branches are associated with radial moments of bulk microscopic

states in the edge region. For integer fillings, we did a straightforward analysis of the large-system limit $R \to \infty$, while in fractional case we studied the $W_\infty$ deformations of incompressible fluid states.

Using these results, we were able to identify Casimir-like ground-state values of charge and conformal spin in the edge theory that depend on the orbital spin, in agreement with the effective field theory approach [21]. This Casimir effect, or chemical potential shift, is irrelevant for a single branch of edge excitations, or for several but independent edge branches, that may occur in the integer Hall effect.

On the contrary, in the case of several interacting branches, such as the hierachical Jain states, these ground-state charge and spin are observable in isolated systems, and are parameterized by the integers $s_i - s_j$, $i,j = 0, 1, \ldots, n-1$. We briefly discussed the Coulomb blockade experiment where the ground-state charge could be measured, while other signatures of this effect remain to be investigated.

Finally, another line of development concerns the subleading terms in the $1/R$ expansion discussed in appendix A, that correspond to non-relativistic corrections of the conformal theory and may give other physical effects parameterized by the orbital spin [10].

## Acknowledgments

The authors would like to thank A G Abanov, D Bernard, A Gromov, T H Hansson, K Jensen, S Klevtsov and P Wiegmann for interesting scientific exchanges. AC acknowledge the hospitality and support by the École Normale Supérieure, Paris, and the G Galilei Institute for Theoretical Physics, Arcetri, where part of this work was done.

## Appendix A. Higher-order terms in the Moyal brackets

The second-order term $O(1/B^2)$ of the Moyal brackets (5.3) for the variation of the first Landau level density takes the form:

$$\delta\widetilde{\rho}^{(0)} = \frac{2\mathrm{i}}{B^2}\left(\bar{\partial}^2\rho^{(0)}\right)\partial^2 w + \text{h.c.}. \tag{A.1}$$

Remembering that $\rho^{(0)} = \rho^{(0)}(r)$, we rewrite it as follows:

$$\delta\widetilde{\rho}^{(0)} = \frac{2\mathrm{i}}{B^2}\left[\left(\frac{\partial}{\partial r^2}\right)^2\rho^{(0)}\right]\left(z^2\partial^2 - \bar{z}^2\bar{\partial}^2\right)w. \tag{A.2}$$

The action of the operator,

$$D_2 = z^2\partial^2 - \bar{z}^2\bar{\partial}^2, \tag{A.3}$$

on a generic polynomial $w \sim z^n\bar{z}^m$ is given by:

$$D_2 z^n\bar{z}^m = (n-m)(n+m-1)\, z^n\bar{z}^m. \tag{A.4}$$

The second-order correction (A.2) to the edge current modes (5.5) can be easily computed by integrating the density in space and by taking the edge limit (5.8); we find:

$$\delta\widetilde{\rho}_k^{(0)} = \frac{1}{R}\int \mathrm{d}x\, x\mathrm{e}^{-2x^2}\,\mathrm{i}D_2 w(x,\theta), \qquad (B=2). \tag{A.5}$$

This expression is different from the leading contribution $\delta\rho_k^{(0)}$ in equation (5.9) for two reasons. The first is the order $O(1/R)$ that is subleading w.r.t. the $O(1)$ behaviour entering the conformal current algebra (3.21). The second aspect is that the dependence on the Fourier modes (A.5) given by the operator $D_2$ does not appear in the conformal operators $\rho_k$ and $L_\kappa$ discussed earlier (see (3.18) and (3.19)). Actually, this spectrum is associated to a higher-spin conserved current of the conformal theory, the dimension-three current $\hat{V}^2(\eta)$, whose expression in the fermionic conformal theory is [32]

$$\hat{V}_0^2 = \frac{1}{R^2}\sum_r \left(r - \frac{1}{2}\right)^2 : \hat{d}_r^\dagger \hat{d}_r : , \tag{A.6}$$

(note the quadratic weight in the sum w.r.t. the linear one of $\hat{L}_0$ (3.18)). Actually, the action of $\hat{V}_0^2$ on a particle-hole excitation, $\hat{d}_n^\dagger \hat{d}_m|\Omega\rangle$ is readily found to reproduce the eigenvalue of $D_2$ in (A.4). The operator $\hat{V}_0^2$ naturally appears as a subleading $1/R^2$ term in the Hamiltonian (3.22) of the conformal theory on the cylinder and corresponds to a non-relativistic correction to the edge dynamics [32]. In summary, the second order term in the Moyal brackets represents a non-relativistic corrections to the conformal theory of edge excitations.

We remark that such a correction is expected to express another physical effect of the orbital spin $s$. The work [10] presented an analysis of the $1/B$ correction to the effective theory of section 2: it involves a spin-two hydrodynamic field in the bulk $b_k = b_{\mu k}\mathrm{d}x^\mu$, where $k$ is a space index, and a generalized action with coupling constant proportional to $s$. In analogy with the discussion in section 2, this action requires a boundary term that involves the edge theory: the corresponding contribution to $\hat{H}$ is expected to be given by (A.6).

In conclusion, the $O(1/B^2)$ term in the Moyal brackets describes a non-relativistic corrections to the conformal theory that is parameterized by the orbital spin. The complete analysis of this effect is left to future developments of this work. Let us mention the related approach [33] discussing the non-relativistic correction to the Hall conductivity due to the orbital spin.

A final remark concerns the relation between the $1/B$ series in the bulk and the $1/R$ expansion at the edge defined in section 3. To leading order in $1/B$, a finite limit is found for bulk quantities in the rescaled coordinate $u$, with $r = Ru \sim \sqrt{N}u$. For example, the limit of the ground-state density of Laughlin states is given by the step function,

$$\rho(\sqrt{N}u) = \frac{\nu B}{2\pi}\Theta(1-u). \tag{A.7}$$

In this limit, the magnetic length is sent to zero, owing to $\ell^2 = 2/B$, and the edge region shrinks to a point. On the contrary, in the edge limit $R \to \infty$ the relevant features take place in the shell $x = r - R = O(\ell)$, where the wavefunctions have support and the Hermite polynomial expansion takes place. This region should be kept finite. Therefore, the $1/B$ approximation is not accurate enough for the analysis of edge excitations because it is too singular in that region.

In conclusion, we identified the first subleading term that is expressed by the spin-three conserved current [32] and parameterized by the orbital spin. Being observable in the conformal theory, such correction could give physical sense to $s$ also for single-branch excitations. The bulk-boundary correspondence for subleading corrections will involve the study of the effective theory introduced in [10] within the multipole expansion of bulk excitations.

## Appendix B. Confining potentials

The simplest model is obtained by adding a quadratic confining potential $V = v|z|^2/R$ to the Landau level Hamiltonian in (3.1), as follows:

$$H^{(2)} = H + V = 2a^\dagger a + 1 + \frac{v}{R}\left(a^\dagger a + b^\dagger b + 1 + a^\dagger b^\dagger + ab\right), \tag{B.1}$$

where $z$ and $\bar{z}$ are expressed in terms of the $a$ and $b$ oscillators (3.2). The exact spectrum of $H$ (B.1) can be obtained by a Bogoliubov transformation in the two-dimensional space of the oscillator pair $(a, b)$, leading to the new pair $(A, B)$ defined by:

$$\begin{cases} A = \cosh(\phi_b)\, a + \sinh(\phi_b)\, b^\dagger, & \text{(B.2)} \\ B = \cosh(\phi_b)\, b + \sinh(\phi_b)\, a^\dagger, & \text{(B.3)} \end{cases}$$

with $\tanh(2\phi_b) = \frac{v}{v+R}$. The result is:

$$H^{(2)} = \left(1 + \sqrt{1 + \frac{2v}{R}}\right) A^\dagger A + \left(\sqrt{1 + \frac{2v}{R}} - 1\right) B^\dagger B + \text{const.}. \tag{B.4}$$

After the transformation, the angular momentum is $J = B^\dagger B - A^\dagger A$, with eigenvalue $m$, and the $A^\dagger A$ eigenvalue $n$ gives the dressed Landau levels energies.

We now obtain the energy spectrum of the edge excitations by evaluating the spectrum of (B.4) in the limit to the edge defined in section three, namely $|z| = r = R + x$, $R \to \infty$ with $m = L + m'$, $L = R^2$, $|m'| < \sqrt{L}$. The result is:

$$\epsilon^{(2)}_{n,m'} = 2n + vR + v\frac{m' + 2n + 1}{R} + O\left(\frac{m'^2}{R^2}\right) + \text{const.}, \tag{B.5}$$

where the constant divergent term must be subtracted from the potential, $V \to V - vR = 2x + x^2/R$, to obtain a finite linear term.

The spectrum with other potentials $V \sim r^k/R^{k-1}$ is necessary to disentangle the contribution of the linear and quadratic terms in the spectrum $\epsilon^{(2)}_{n,m}$ and to evaluate the higher terms $x^3/R^2$, etc... . The Bogoliubov transformation does not apply to generic potentials, and we use another method that works in the relevant limit $R \to \infty$. Note that the angular momentum $J = b^\dagger b - a^\dagger a$ is a good quantum number for any potential and it takes very large values in this limit; this means that the expectation values of $b^\dagger b$ is of order $R^2$. Remembering the case of Bose–Einstein condensation, we can treat the $b$ operator as a classical variable, and write:

$$b \sim b^\dagger \sim \sqrt{b^\dagger b} = \sqrt{R^2 + m' + a^\dagger a} \simeq R\left(1 + \frac{m' + a^\dagger a}{2R^2}\right) \sim R + O\left(\frac{1}{R}\right). \tag{B.6}$$

We use this approximation in the original Hamiltonian (B.1) and find the expression:

$$H^{(2)} = 2\left(1 + \frac{v}{R}\right) a^\dagger a + v\frac{m'}{R} + v\left(a^\dagger + a\right) + \text{const.}. \tag{B.7}$$

This result can be checked with the $R \to \infty$ limit of the Bogoliubov transformation (B.2) and (B.3). Note that the rotation angle $\phi_b$ is small:

$$\begin{cases} A \simeq a + \frac{v}{2R} b^\dagger, & \text{(B.8)} \\ B \simeq b + \frac{v}{2R} a^\dagger. & \text{(B.9)} \end{cases}$$

Substituting these expressions and the approximation (B.6) into the exact result (B.4), we reobtain the expression (B.7). Furthermore, the result (B.7) also agrees with the $R \to \infty$ limit of the exact matrix elements of the quadratic potential,

$$\begin{aligned}&\langle i, R^2 + m' | V^{(2)} | j, R^2 + m' \rangle \\ &\simeq v \left[ \left( R + \frac{m' + 2i + 1}{R} \right) \delta_{i,j} + \sqrt{j+1}\delta_{i,j+1} + \sqrt{j}\delta_{i,j-1} \right],\end{aligned} \tag{B.10}$$

that can be evaluated using the wave functions (3.3) and the help of Mathematica.

We now diagonalize the approximate $H^{(2)}$ (B.7) directly. We note that a shift of the operator $a$ by a constant, setting

$$A = a + \frac{v}{2}\left(1 - \frac{v}{R}\right), \tag{B.11}$$

reproduces the $R \to \infty$ limit of the Bogoliubov transformation (B.4). In conclusion, the spectrum (B.5) has been recovered by using directly the approximation (B.6) in the Hamiltonian $H^{(2)}$.

We extend the previous analysis to the cases of linear and quartic confining potentials, $V^{(1)} = v_1 r$ and $V^{(4)} = v_4 r^4/R^3$. In the linear case, the Hamiltonian is:

$$H^{(1)} = 2a^\dagger a + 1 + \frac{v_1}{R}\left(a^\dagger a + b^\dagger b + 1 + a^\dagger b^\dagger + ab\right)^{1/2}. \tag{B.12}$$

We apply the large $R$ limit and the approximation (B.6), subtract the infinite term and find:

$$H^{(1)} = 2a^\dagger a + \frac{v_1}{2}\left(a^\dagger + a\right) + \frac{v_1}{8R}\left(6a^\dagger a + 4m'\right) - \frac{v_1}{8R}\left(a^{\dagger 2} + a^2\right) + \text{const.}. \tag{B.13}$$

The calculation of the matrix elements of $V^{(1)}$ in the edge limit agrees with the previous result:

$$\begin{aligned}&\langle i, R^2 + m' | V^{(1)} | j, R^2 + m' \rangle \\ &\simeq v_1 \left[ \left( \frac{6i + 4m'}{8R} + R \right) \delta_{i,j} + \frac{v_1}{2}\left( \sqrt{i-1}\delta_{i-1,j} + \sqrt{i}\delta_{i,j-1} \right) \right. \\ &\left. + \frac{v_1}{8R}\left( \sqrt{(j+2)(j+1)}\delta_{i,j+2} + \sqrt{j(j-1)}\delta_{i,j-2} \right) \right].\end{aligned} \tag{B.14}$$

The equation (B.13) involves an additional term $\left(a^{\dagger 2} + a^2\right)$ w.r.t the quadratic case (B.7) corresponding to non-vanishing matrix elements on the third diagonal. After the shift by constant of the operator $a$, the Hamiltonian $H^{(1)} \sim A^\dagger A + \lambda\left(A^{\dagger 2} + A^2\right)$ can be diagonalized by a change of the oscillator frequency which turns out to be $O(1/R^2)$. The diagonal form of the Hamiltonian $H^{(1)}$ is finally,

$$H^{(1)} \simeq \left(2 + \frac{3v_1}{4R}\right) A^\dagger A + v_1 \frac{m'}{2R} + \text{const.}, \tag{B.15}$$

with spectrum:

$$\epsilon^{(1)}_{n,m'} = 2n + v_1\left(\frac{m'}{2R} + \frac{3n}{4R}\right) + \text{const.}. \tag{B.16}$$

In the case of quartic potential, the approximated Hamiltonian can be written as follows:

$$H^{(4)} = 2a^\dagger a + 1 + \frac{v_4}{R}\left(6a^\dagger a + 2m'\right) + 2v_4\left(a^\dagger + a\right) + \frac{v_4}{R}\left(a^{\dagger 2} + a^2\right) + \text{const.}, \tag{B.17}$$

in agreement with the matrix elements,

$$\begin{aligned}&\langle i, R^2+m'|V^{(4)}|j, R^2+m'\rangle\\&\simeq v_4\left[\frac{1}{R}\left(6i+2m'+\text{const.}\right)\delta_{i,j}+2\sqrt{j+1}\delta_{i,j+1}+2\sqrt{j}\delta_{i,j-1}\right.\\&\left.+\frac{1}{R}\left(\sqrt{(j+1)\,(j+2)}\delta_{i,j+2}+\sqrt{j\,(j-1)}\delta_{i,j-2}\right)\right].\end{aligned}\tag{B.18}$$

We can diagonalized (B.17) by introducing once again a constant shift in operator $a$ and the frequency redefinition, leading to the spectrum:

$$\epsilon^{(4)}_{n,m'}=2n+v_4\left(\frac{2m'}{R}+\frac{6n}{R}\right)+\text{const.}.\tag{B.19}$$

Now let us discuss the generic confining potential (4.2) for $r=R+x\to\infty$:

$$V(x;R)=a_1x+\frac{a_2}{R}x^2+\frac{a_3}{R^2}x^3+\dots.\tag{B.20}$$

We are interested in the relativistic conformal spectrum at the edge (4.1), which is of order $O(1/R)$. We compare the spectrum of $V^{(2)}$, $V^{(1)}$ and $V^{(4)}$ computed in this limit and obtain the following consistent result for the spectrum:

$$\epsilon_{n,m'}=a_1\left(\frac{m'}{2R}+\frac{3n}{4R}\right)+a_2\frac{n}{2R}+\text{const.}.\tag{B.21}$$

This comparison shows that the higher terms $x^3/R^2$ that appear for example in $V^{(4)}$, do not contribute to leading order $O(1/R)$. This fact can also be checked by evaluating the corresponding matrix elements in the edge limit (3.9).

In conclusion, the relativistic conformal spectrum takes values from the linear and quadratic terms in (B.20).

## ORCID iDs

Andrea Cappelli https://orcid.org/0000-0003-1306-4698

## References

[1] Avron J E, Seiler R and Zograf P G 1995 Viscosity of quantum Hall fluids *Phys. Rev. Lett.* **75** 697
[2] Wen X G 2007 *Quantum Field Theory of Many-body Systems* (Oxford: Oxford University Press)
[3] Read N 2009 Non-Abelian adiabatic statistics and Hall viscosity in quantum Hall states and $p(x)+\mathrm{i}p(y)$ paired superfluids *Phys. Rev.* B **79** 045308
Read N and Rezayi E H 2011 Hall viscosity, orbital spin, and geometry: paired superfluids and quantum Hall systems *Phys. Rev.* B **84** 085316
Bradlyn B, Goldstein M and Read N 2012 Kubo formulas for viscosity: Hall viscosity, Ward identities, and the relation with conductivity *Phys. Rev.* B **86** 245309
[4] Haldane F D M 2009 'Hall viscosity', intrinsic metric of incompressible fractional Hall fluids (arXiv:0906.1854)
Haldane F D M 2011 Geometrical description of the fractional quantum Hall effect *Phys. Rev. Lett.* **107** 116801
Haldane F D M 2011 Self-duality and long-wavelength behavior of the Landau-level guiding-center structure function, and the shear modulus of fractional quantum Hall fluids (arXiv:1112.0990)

Park Y and Haldane F D M 2014 Guiding-center Hall viscosity and intrinsic dipole moment along edges of incompressible fractional quantum Hall fluids *Phys. Rev.* B **90** 045123
[5] Wen X G and Zee A 1992 Shift and spin vector: new topological quantum numbers for the Hall fluids *Phys. Rev. Lett.* **69** 953
Wen X G and Zee A 1992 Shift and spin vector: new topological quantum numbers for the Hall fluids *Phys. Rev. Lett.* **69** 3000
Fröhlich J and Studer U M 1993 Gauge invariance and current algebra in nonrelativistic many body theory *Rev. Mod. Phys.* **65** 733
[6] Abanov A G and Gromov A 2014 Electromagnetic and gravitational responses of two-dimensional noninteracting electrons in a background magnetic field *Phys. Rev.* B **90** 014435
[7] Bradlyn B and Read N 2015 Topological central charge from Berry curvature: gravitational anomalies in trial wave functions for topological phases *Phys. Rev.* B **91** 165306
Laskin M, Chiu Y H, Can T and Wiegmann P 2016 Emergent conformal symmetry of quantum Hall states on singular surfaces *Phys. Rev. Lett.* **117** 266803
[8] Klevtsov S and Wiegmann P 2015 Geometric adiabatic transport in quantum Hall states *Phys. Rev. Lett.* **115** 086801
Can T, Laskin M and Wiegmann P 2015 Geometry of quantum Hall states: gravitational anomaly and kinetic coefficients *Ann. Phys.* **362** 752
[9] Wiegmann P B 2013 Hydrodynamics of Euler incompressible fluid and the fractional quantum Hall effect *Phys. Rev.* B **88** 241305
Wiegmann P B and Abanov A G 2014 Anomalous hydrodynamics of two-dimensional vortex fluids *Phys. Rev. Lett.* **113** 034501
Wiegmann P B 2018 Nonlinear waves of fractional quantum Hall states as an evidence of the gravitational anomaly *Phys. Rev. Lett.* **120** 08660
[10] Cappelli A and Randellini E 2016 Multipole expansion in the quantum Hall effect *J. High Energy Phys.* JHEP03(2016)105
[11] Gromov A and Bradlyn B 2017 Investigating anisotropic quantum Hall states with bimetric geometry *Phys. Rev. Lett.* **119** 146602
Gromov A and Bradlyn B 2017 Investigating anisotropic quantum Hall states with bimetric geometry *Phys. Rev. Lett.* **119** 189901
Gromov A and Son D T 2017 Bimetric theory of fractional quantum Hall states *Phys. Rev.* X **7** 041032
[12] Cappelli A, Dunne G V, Trugenberger C A and Zemba G R 1993 Conformal symmetry and universal properties of quantum Hall states *Nucl. Phys.* B **398** 531
[13] Laughlin R B Quantized Hall conductivity in two-dimensions *Phys. Rev. Lett.* B **23** 5632
[14] Di Francesco P, Mathieu P and Sénéchal D 1997 *Conformal Field Theory* (New York: Springer)
[15] Read N and Green D 2000 Paired states of fermions in two-dimensions with breaking of parity and time reversal symmetries, and the fractional quantum Hall effect *Phys. Rev.* B **61** 10267
Cappelli A, Huerta M and Zemba G R 2002 Thermal transport in chiral conformal theories and hierarchical quantum Hall states *Nucl. Phys.* B **636** 568
[16] Banerjee M, Heiblum M, Rosenblatt A, Oreg Y, Feldman D E, Stern A and Umansky V 2017 Observed quantization of anyonic heat flow *Nature* **545** 75
[17] Stone M 2012 Gravitational anomalies and thermal Hall effect in topological insulators *Phys. Rev.* B **85** 184503
Abanov A G and Gromov A 2014 Thermal Hall effect and geometry with torsion *Phys. Rev. Lett.* **114** 016802
[18] Abanov A G and Gromov A 2014 Density-curvature response and gravitational anomaly *Phys. Rev. Lett.* **113** 266802
[19] Hoyos C and Son D T 2012 Hall viscosity and electromagnetic response *Phys. Rev. Lett.* **108** 066805
[20] Can T, Forrester P J, Téllez G and Wiegmann P 2014 Singular behavior at the edge of Laughlin states *Phys. Rev.* B **89** 235137
[21] Gromov A, Jensen K and Abanov A G 2016 Boundary effective action for quantum Hall states *Phys. Rev. Lett.* **116** 126802
[22] Cappelli A, Trugenberger C A and Zemba G R 1993 Infinite symmetry in the quantum Hall effect *Nucl. Phys.* B **396** 465
[23] Iso S, Karabali D and Sakita B 1992 Fermions in the lowest Landau level: bosonization, W infinity algebra, droplets, chiral bosons *Phys. Lett.* B **296** 143

Iso S, Karabali D and Sakita B 1992 One-dimensional fermions as two-dimensional droplets via Chern–Simons theory *Nucl. Phys.* B **388** 700
[24] Cappelli A, Trugenberger C A and Zemba G R 1993 Large N limit in the quantum Hall effect *Phys. Lett.* B **306** 100
[25] Ilan R, Grosfeld E and Stern A 2008 Coulomb blockade as a probe for non-Abelian statistics in Read–Rezayi states *Phys. Rev. Lett.* **100** 086803
Cappelli A, Georgiev L S and Zemba G R 2009 Coulomb blockade in hierarchical quantum Hall droplets *J. Phys. A: Math. Theor.* **42** 222001
[26] Agam O, Bettelheim E, Wiegmann P and Zabrodin A 2002 Viscous fingering and a shape of an electronic droplet in the quantum Hall regime *Phys. Rev. Lett.* **88** 236801
[27] Gromov A, Cho G Y, You Y, Abanov A G and Fradkin E 2015 Framing anomaly in the effective theory of the fractional quantum Hall effect *Phys. Rev. Lett.* **114** 016805
[28] Dunne G V 1994 Edge asymptotics of planar electron densities *Int. J. Mod. Phys.* B **8** 1625
[29] de Chamon C C and Wen X G 1994 Sharp and smooth boundaries of quantum Hall liquids *Phys. Rev.* B **49** 8227
Wang J, Meir Y and Gefen Y 2013 Edge reconstruction in the $\nu = 2/3$ fractional quantum Hall state *Phys. Rev. Lett.* **111** 246803
[30] Girvin S M, MacDonald A H and Platzman P M 1986 Magneto-roton theory of collective excitations in the fractional quantum Hall effect *Phys. Rev.* B **33** 2481
[31] Jain J K 2007 *Composite Fermions* (Cambridge: Cambridge University Press)
[32] Cappelli A, Trugenberger C A and Zemba G R 1996 W(1 + infinity) dynamics of edge excitations in the quantum Hall effect *Ann. Phys.* **246** 86
[33] Moroz S, Hoyos C and Radzihovsky L 2015 Galilean invariance at quantum Hall edge *Phys. Rev.* B **91** 195409
Moroz S, Hoyos C and Radzihovsky L 2015 Galilean invariance at quantum Hall edge *Phys. Rev.* B **91** 199906 (erratam)
Moroz S, Hoyos C and Radzihovsky L 2017 Galilean invariance at quantum Hall edge *Phys. Rev.* B **96** 039902
Höller J and Read N 2016 Comment on âĂIJ-Galilean invariance at quantum Hall edge *Phys. Rev.* B **93** 197401